J. Fluid Mech. (1988), *vol.* 193, *pp.* 533–568
Printed in Great Britain

First-order wall curvature effects upon the Stokes resistance of a spherical particle moving in close proximity to a solid wall

By ADEBOWALE FALADE† AND HOWARD BRENNER‡

† Faculty of Engineering, Technology and Environmental Sciences, Lagos State University, Badagry Expressway, P.M.B. 1087, Apapa, Lagos State, Nigeria

‡ Department of Chemical Engineering, Massachusetts Institute of Technology, Cambridge, MA 02139, USA

(Received 24 April 1987 and in revised form 22 December 1987)

A method for calculating the effect of the curvature of a solid wall bounding a viscous fluid upon the quasi-static Stokes force $\boldsymbol{F}$ and torque $\boldsymbol{T}$ experienced by a spherical particle performing arbitrarily directed translational and rotational motions in close proximity to the wall is given. The results presented herein are valid for values of the ratio $\kappa = a/d$ (a = sphere radius, d = shortest perpendicular distance from the sphere centre to the wall) over the entire range $0 \leqslant \kappa \leqslant 1$, provided that $\beta = a/R_0 \ll 1$ and, simultaneously, $d/R_0 \equiv \beta/\kappa \ll 1$ (R_0 = characteristic radius of curvature of the wall). Unlike existing wall-effect theories, our results are valid for $\kappa = O(1)$. It is shown that to the first-order in β (and, concomitantly, in d/R_0), wall curvature effects upon $\boldsymbol{F}$ and $\boldsymbol{T}$ depend linearly upon two scalar principal curvature coefficients of the wall at the foot of the shortest normal to the wall from the sphere centre. This single-particle analysis is used to resolve a 'paradox' relating to macroscopic slip boundary conditions prevailing at a wall bounding a dilute ferrofluid suspension undergoing rotation relative to a magnetic field.

1. Introduction

The problem of calculating the increased Stokes resistance of a spherical particle moving proximate to a wall has a long history dating back nearly a century to Lorentz (1896) for plane walls and to Ladenburg (1907) for circular cylindrical walls. Reviews which summarize most of the significant studies to date are available in Happel & Brenner (1965), Brenner (1966, 1972), Goldsmith & Skalak (1975), Leal (1980), Hasimoto & Sano (1980), O'Neill & Ranger (1982) and Hirschfeld, Brenner & Falade (1984).

For the case $\kappa = a/d \ll 1$ and $\beta = a/R_0 \ll 1$ (where a = sphere radius, d = shortest normal distance from the sphere's centre to the wall, R_0 = characteristic radius of curvature of wall), Cox & Brenner's (1967*a*) analysis provides a general method for determining the Stokes resistance of the sphere. However, their results may fail to yield convergent expressions when $d/R_0 \equiv \beta/\kappa \ll 1$ (Hirschfeld *et al.* 1984). This convergence problem can be avoided by employing the asymptotic scheme of Falade & Brenner (1985) jointly with certain results of Hirschfeld *et al.* (1984).

For circumstances where $\kappa = O(1)$, most analyses (of the $d/R_0 \ll 1$ case) treat only the problem of a *plane* wall, corresponding to $R_0 = \infty$ (Brenner 1961; Dean & O'Neill 1963; O'Neill 1964; Cox & Brenner 1967*b*; Cooley & O'Neill 1968; Lee & Leal 1980, to cite a few). Among the studies of sphere motions occurring nearby to *curved*

boundaries are those of: (i) Jeffery (1915), Stimson & Jeffery (1926), Majumdar (1965, 1967), O'Neill (1969), Cooley & O'Neill (1969*a*, *b*), Davis (1969), O'Neill & Majumdar (1970*a*, *b*) and Cooley (1971), who collectively calculated the resistances of two proximate spheres (equal or unequal) performing arbitrarily directed relative translational or rotational motions; (ii) Bungay & Brenner (1973) and Cox (1974), in which 'lubrication-theory'-like singular perturbation techniques were employed to analyse the narrow-gap case, $\kappa \to 1$, for the case of non-spherical and non-planar bounding walls; (iii) Gluckman, Pfeffer & Weinbaum (1971) and Leichtberg, Pfeffer & Weinbaum (1976), in which a numerical scheme was used to calculate the axisymmetric flow past concentrically positioned spheres, spheroids and clusters of spheres enclosed within a circular cylinder; (iv) Lee & Leal (1982), who numerically calculated the resistance of a sphere in the presence of a *deformable* interface.

This paper describes an asymptotic scheme for calculating first- and higher-order wall curvature effects upon the Stokes resistance of a sphere for the dual range $\kappa = O(1)$ and $d/R_0 \ll 1$ (though, in fact, we shall only bring the calculations to fruition here to the first-order in d/R_0). Previous practice has been to employ the sphere/plane-wall results (Lee & Leal 1980) whenever wall effects were required for $\kappa = O(1)$, even when the boundaries were, in fact, (slightly) curved. But, as observed by Brenner (1984) in commenting upon classes of $d/R_0 \ll 1$ problems involving the motion of spherical particles proximate to curved walls, 'paradoxical' results may arise in applications. This occurs when attempts are made to asymptotically compare results derived for the $\kappa \ll 1$ case with corresponding ones derived from sphere/plane-wall solutions for the $\kappa = O(1)$ case. In particular, it was observed that no common overlap region exists between these two alternative $d/R_0 \ll 1$ solutions, and hence that a smooth transition between the $\kappa \ll 1$ and $\kappa = O(1)$ cases apparently fails to exist, even with regard to the algebraic signs of the hydrodynamic coupling coefficients connecting the translational and rotational motions of the sphere.

Resolution of this 'paradox' is achieved herein by demonstrating that proper matching between the outer ($\kappa \ll 1$) and inner [$\kappa = O(1)$] regions requires more than the superficial considerations heretofore addressed to this $d/R_0 \ll 1$ case. In a sense the problem is a classical one in the theory of matched asymptotic expansions for situations in which there exist not one, but rather two small (non-dimensional) parameters characterizing the problem, these being $a/R_0 \ll 1$ and $d/R_0 \ll 1$ in the present case.

A summary of the general contents of the paper now follows. In §2 we formulate the Stokes flow problem for a translating–rotating sphere moving in close proximity ($d/R_0 \ll 1$) to a curved solid wall. An asymptotic solution scheme is formulated in §3. Explicit expressions are derived in §4 for first-order wall curvature effects upon the Stokes force and torque. These results are used in §5 to determine the resistance of a proximate sphere of radius a translating and rotating internally or externally to a spherical wall of relatively large curvature R_0 for the case where $\beta = a/R_0 \ll 1$. These asymptotic spherical-wall results are compared with known exact bipolar- or tangent-sphere-coordinate-derived sphere/sphere results (valid for *all* physically possible β) for both the interior and exterior cases. Finally, §6 applies our asymptotic results to the case of a relatively small spherical particle moving nearby to the wall of a large circular cylinder. Thereby, the $d/R_0 \ll 1$ 'paradox' that spawned this study is resolved by demonstrating the existence of an asymptotic regime in which the $\kappa \ll 1$ and $\kappa = O(1)$ solutions are satisfactorily matched, resulting in a smooth transition between the two.

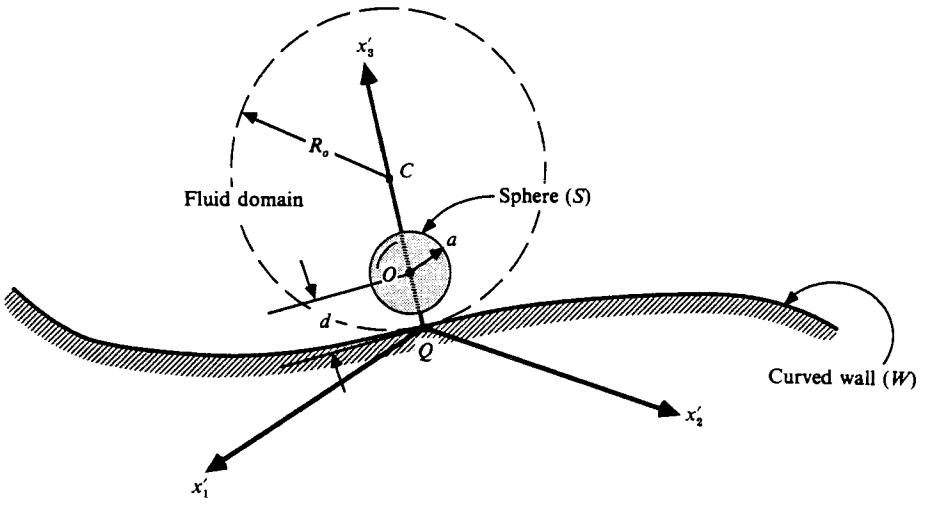

FIGURE 1. Spherical particle S near a slightly curved wall W. Definition sketch.

2. Formulation

Consider a sphere (S) of radius a translating and rotating 'slowly' in an otherwise quiescent viscous fluid (with respective velocities U_i' and Ω_i') in proximity to an arbitrarily curved solid wall (W) (figure 1). Let the characteristic radius of curvature R_o of the wall in the immediate proximity of the sphere be such that $1 \gg a/R_o$ ($=\beta$, say), and let the sphere centre O be momentarily at the point $(0, 0, d)$ relative to a Cartesian coordinate system (x_1', x_2', x_3') whose origin Q lies at the foot of the shortest possible normal to W passing through O. Additionally, let the coordinate surface $x_3' = 0$, which contains the x_1' and x_2' axes, be the tangent plane of W at Q. As in the sketch shown in figure 1, we shall always choose the positive x_3' axis to lie along the line drawn from Q through the sphere centre O, irrespective of whether the sphere S lies external or internal to the surface $x_3' = \bar{f}(x_1', x_2')$ describing the wall W.

For now, no restriction will be placed on the ratio $\kappa = a/d$ other than $0 \leqslant \kappa \leqslant 1$. However, we shall require that, like a/R_o, d/R_o satisfy the inequality $d/R_o \ll 1$. It will be assumed that the respective domains of x_1' and x_2' spanned by the wall lie in the bounded regions $-\delta_\alpha' \leqslant x_\alpha' \leqslant \gamma_\alpha'$ ($\alpha = 1, 2$), where $|\delta_\alpha'|$ and $|\gamma_\alpha'|$ are each much greater than a and d.

We seek to determine the fluid velocity v_i' ($i = 1, 2, 3$) and pressure p' generated by the sphere's motion. Though this flow is generally unsteady, we shall nevertheless suppose the fluid motion to be governed by the quasi-steady Stokes equations

$$\mu v_{i,jj}' - p_{,i}' = 0 \tag{2.1}$$

and

$$v_{j,j}' = 0. \tag{2.2}$$

These are to be solved subject to the boundary conditions

$$v_i' = U_i' + \epsilon_{ijk}\Omega_j' \bar{x}_k' \quad \text{on } r'^2 \overset{\text{def}}{=} x_1'^2 + x_2'^2 + (x_3' - d)^2 = a^2, \tag{2.3a}$$

$$v_i' = 0 \quad \text{on } x_3' = \bar{f}(x_1', x_2'), \quad (\delta_1' \leqslant x_1' \leqslant \gamma_1', \quad \delta_2' \leqslant x_2' \leqslant \gamma_2'), \tag{2.3b}$$

$$v_i' \to 0 \quad \text{as } |r'| \to \infty. \tag{2.3c}$$

Here, $\bar{x}_k' = x_k' - d\delta_{k3}$. Note that (2.3*c*) need not be satisfied in circumstances where W completely encloses S.

In terms of dimensionless quantities defined as

$$\left.\begin{aligned} \tilde{v}_i &= \frac{v_i'}{U_o}, \quad \tilde{U}_i = \frac{U_i'}{U_o}, \quad \tilde{\Omega}_i = \frac{\Omega_i' R_o}{U_o}, \quad \tilde{p} = \frac{p' R_o}{\mu U_o}, \\ \tilde{x}_i &= \frac{x_i'}{R_o}, \quad \tilde{r} = \frac{r'}{R_o}, \quad \tilde{\delta}_\alpha = \frac{\delta_\alpha'}{R_o}, \quad \tilde{\gamma}_\alpha = \frac{\gamma_\alpha'}{R_o} \end{aligned}\right\} \tag{2.4}$$

($\alpha = 1, 2$), (with U_o a characteristic particle velocity), the preceding system of equations becomes

$$\tilde{v}_{i,jj} - \tilde{p}_{,i} = 0, \tag{2.5}$$

$$\tilde{v}_{j,j} = 0, \tag{2.6}$$

$$\tilde{v}_i = \tilde{U}_i + \epsilon_{ijk}\tilde{\Omega}_j \tilde{\bar{x}}_k \quad \text{on } \tilde{r}^2 \overset{\text{def}}{=} \tilde{x}_1^2 + \tilde{x}_2^2 + (\tilde{x}_3 - \beta\kappa^{-1})^2 = \beta^2, \tag{2.7}$$

$$\tilde{v}_i = 0 \quad \text{on } \tilde{x}_3 = \tilde{f}(\tilde{x}_1, \tilde{x}_2), \quad (\tilde{\delta}_1 \leqslant \tilde{x}_1 \leqslant \tilde{\gamma}_1, \quad \tilde{\delta}_2 \leqslant \tilde{x}_2 \leqslant \tilde{\gamma}_2), \tag{2.8}$$

$$\tilde{v}_i \to 0 \quad \text{as } |\tilde{r}| \to \infty. \tag{2.9}$$

Again, (2.9) is enforced only if the wall does not completely enclose the sphere. In (2.7), $\tilde{\bar{x}} = \tilde{x}_k - \beta\kappa^{-1}\delta_{k3}$.

The boundary-value problem posed by (2.5)–(2.9) does not lend itself to exact analytical solution except in the special cases where W is such as to permit the use of bipolar coordinates, namely: (i) $\tilde{f}(\tilde{x}_1, \tilde{x}_2) = 0$, corresponding to a plane wall (cf. the list of references for this case cited earlier); and (ii) the curved boundary W is itself a spherical surface (cf. earlier references thereto). An asymptotic solution is proposed in the next section for the case where $d/R_o \equiv \beta\kappa^{-1} \ll 1$, with κ of order unity or smaller.

It will be assumed henceforth that $\tilde{f}(\tilde{x}_1, \tilde{x}_2)$ is an analytic function at Q and, if more than one normal can be drawn through the sphere centre O from W, that the shortest such normal distance is much smaller in length than the others. By virtue of the definition of the coordinate system, the Taylor series expansion of $\tilde{f}$ about Q is

$$\tilde{f}(\tilde{x}_1, \tilde{x}_2) = \tfrac{1}{2}\alpha_{ij}\tilde{x}_j\tilde{x}_i + \tfrac{1}{6}\alpha_{ijk}\tilde{x}_k\tilde{x}_j\tilde{x}_i + \ldots, \tag{2.10a}$$

where

$$\alpha_{ij} = \frac{\partial^2 \tilde{f}}{\partial\tilde{x}_i\,\partial\tilde{x}_j}, \quad \alpha_{ijk} = \frac{\partial^3 \tilde{f}}{\partial\tilde{x}_i\,\partial\tilde{x}_j\,\partial\tilde{x}_k}, \text{ etc.} \tag{2.10b,c}$$

($i, j, k = 1, 2$). If the surface is sufficiently regular at Q, then $\alpha_{12} = \alpha_{21}$ and $\alpha_{iji} = \alpha_{jii} = \alpha_{iij}$ (no sum on i). Moreover, it is always possible to orient the $\tilde{x}_1$ and $\tilde{x}_2$ axes such that $\alpha_{12} = \alpha_{21} = 0$, corresponding to choosing the principal axes of curvature† at Q for the definitions of these Cartesian axes.

2.1. *Perturbation expansions for $\tilde{v}_i$ and $\tilde{p}$*

Upon suppressing the wall 'curvature' tensors $\alpha_{jk}, \alpha_{jkl}, \ldots$ from the arguments of the respective fields $\tilde{v}_i(\tilde{\boldsymbol{x}}; \beta; \kappa; \alpha_{jk}; \alpha_{jkl}; \ldots)$ and $\tilde{p}(\tilde{\boldsymbol{x}}; \beta; \kappa; \alpha_{jk}; \alpha_{jkl}; \ldots)$ [with $\tilde{\boldsymbol{x}} \equiv (\tilde{x}_1, \tilde{x}_2,$

† Because of our arbitrary sign convention in figure 1 regarding the direction of x_3' with respect to the concavity or convexity of W at Q, the dyadic α_{ij} may differ by an algebraic sign from the usual curvature dyadic $-\nabla_{\text{II}}\boldsymbol{n}$ [with $\nabla_{\text{II}} = (\boldsymbol{I} - \boldsymbol{nn})\cdot\nabla$ the surface gradient operator] (Gibbs & Wilson 1960; Weatherburn 1927; Misner, Thorne & Wheeler 1973), according to the so-called 'positive' unit normal vector $\boldsymbol{n}$ to W at Q lies parallel or antiparallel to the unit vector $\boldsymbol{i}_3'$. Despite this ambiguity, we shall nevertheless refer to α_{ij} as the curvature dyadic.

$\tilde{x}_3)]$ satisfying (2.5)–(2.10), we shall henceforth assume – subject to *a posteriori* verification – the existence of a solution of this system of equations of the form

$$\tilde{v}_i(\tilde{\boldsymbol{x}};\beta;\kappa) = {}_0v_i(\boldsymbol{x};\kappa)+\beta\,{}_1v_i(\boldsymbol{x};\kappa)+\beta^2\,{}_2v_i(\boldsymbol{x};\kappa)+\ldots, \tag{2.11}$$

$$\tilde{p}(\tilde{\boldsymbol{x}};\beta;\kappa) = \beta^{-1}\,{}_0p(\boldsymbol{x};\kappa)+{}_1p(\boldsymbol{x};\kappa)+\beta\,{}_2p(\boldsymbol{x};\kappa)+\ldots, \tag{2.12}$$

in which $x_i \overset{\text{def}}{=} \beta^{-1}\tilde{x}_i$ $(i = 1,2,3)$ are 'stretched' variables. As indicated by the notation, the wall 'curvature' tensor coefficients $\alpha_{jk}, \alpha_{jkl}, \ldots$ have been explicitly suppressed in the arguments of the perturbation fields ${}_nv_i$, ${}_np$ $(n = 0,1,2,\ldots)$ appearing on the right-hand sides of the above equations, although they are understood to be *implicitly* present. When expressed in terms of the stretched coordinates $\boldsymbol{x} \equiv (x_1, x_2, x_3)$, these perturbation fields will be shown to be independent of β, as already suggested by the explicit absence of β from the arguments of these fields.

In terms of the stretched independent variables x_i, (2.10) may be rewritten in the form

$$x_3 = f(x_1,x_2) = \tfrac{1}{2}\beta\alpha_{ij}x_jx_i+\tfrac{1}{6}\beta^2\alpha_{ijk}x_kx_jx_i+O(\beta^3), \tag{2.13a}$$

where

$$\alpha_{ij} = \frac{\partial^2 f}{\partial x_i\,\partial x_j}, \quad \alpha_{ijk} = \frac{\partial^3 f}{\partial x_i\,\partial x_j\,\partial x_k}, \text{ etc.} \tag{2.13b,c}$$

The wall boundary condition (2.8) may be transferred to the plane $x_3 = 0$ by expanding $\tilde{v}_i$ in a Taylor series about $x_3 = 0$. Taking into account the asymptotic form (2.11) for $\tilde{v}_i$, such an expansion leads to the expression

$$\begin{aligned}{}_0v_i+\beta[\tfrac{1}{2}\alpha_{km}x_mx_k\,{}_0v_{i,3}+{}_1v_i]+\beta^2[\tfrac{1}{6}\alpha_{jkm}x_mx_kx_j\,{}_0v_{i,3}\\ +\tfrac{1}{8}(\alpha_{km}x_mx_k)^2\,{}_0v_{i,33}+\tfrac{1}{2}\alpha_{km}x_mx_k\,{}_1v_{i,3}+{}_2v_i]+O(\beta^3) = 0.\end{aligned} \tag{2.14}$$

Provided that $\beta \ll 1$, equation (2.14) closely approximates (2.8). When (2.11) and (2.12) are substituted into (2.5)–(2.7), and terms of like order in β collected together, the following ordered sets of perturbation equations and boundary conditions result:

2.1.1. *Zero-order equations*

$$-{}_0p_{,i}+{}_0v_{i,jj} = 0, \quad {}_0v_{j,j} = 0, \tag{2.15a,b}$$

$${}_0v_i = U_i+\epsilon_{ijk}\Omega_j\bar{x}_k \quad \text{on } r^2 \overset{\text{def}}{=} x_1^2+x_2^2+(x_3-\kappa^{-1})^2 = 1, \tag{2.16}$$

$${}_0v_i = 0 \quad \text{on } x_3 = 0, \tag{2.17}$$

$${}_0v_i \to 0 \quad \text{as } |r| \to \infty, \tag{2.18}$$

where $\bar{x}_k = x_k-\kappa^{-1}\delta_{k3}$ in (2.16).

2.1.2. *First-order equations*

$$-{}_1p_{,i}+{}_1v_{i,jj} = 0, \quad {}_1v_{j,j} = 0, \tag{2.19a,b}$$

$${}_1v_i = 0 \quad \text{on } x_1^2+x_2^2+(x_3-\kappa^{-1})^2 = 1, \tag{2.20}$$

$${}_1v_i = -\tfrac{1}{2}\alpha_{km}x_mx_k\,{}_0v_{i,3} \quad \text{on } x_3 = 0, \tag{2.21}$$

$${}_1v_i \to 0 \quad \text{as } |r| \to \infty. \tag{2.22}$$

From (2.15*b*) and (2.17) it follows that

$${}_1v_3 = 0 \quad \text{on } x_3 = 0.$$

2.1.3. *Second-order equations*

$$ {}_2v_{i,jj} - {}_2p_{,i} = 0, \quad {}_2v_{j,j} = 0, \tag{2.23a,b} $$

$$ {}_2v_1 = 0 \quad \text{on } x_1^2 + x_2^2 + (x_3 - \kappa^{-1})^2 = 1, \tag{2.24} $$

$$ {}_2v_i = -\tfrac{1}{2}\alpha_{km}\, x_m\, x_k\, {}_1v_{i,3} - \tfrac{1}{2}(\tfrac{1}{2}\alpha_{km}\, x_m\, x_k)^2\, {}_0v_{i,33} - \tfrac{1}{6}\alpha_{jkm}\, x_m\, x_k\, x_j\, {}_0v_{i,3} \quad \text{on } x_3 = 0, \tag{2.25} $$

$$ {}_2v_i \to 0 \quad \text{as } |r| \to \infty. \tag{2.26} $$

'Far-field' boundary conditions such as are embodied in (2.18), (2.22) and (2.26), which require the vanishing of the perturbation velocity field ${}_nv_i$ ($n = 0, 1, 2, \ldots$) at 'infinity', do not derive from (2.9) in circumstances where the curved wall W partially or completely encloses the sphere S. (For example, W may be either an infinitely long or finite-length circular cylinder containing S in its interior.) Rather, these far-field boundary conditions represent a transference to infinity of the original, exactly posed, zero-velocity, no-slip boundary condition imposed upon the second branch of W (e.g. the opposite side of the circular cylinder), which is physically situated at a finite distance from the sphere. Formal details confirming the legitimacy of this far-field transference to infinity can be found in our earlier contribution (Falade & Brenner 1985; see equations (2.5) and (2.11) of that paper).

3. Solution

3.1. *Zero-order solution*

It can be readily deduced from the analysis of Lee & Leal (1980) that a general solution of (2.15a) in spherical bipolar coordinates (ξ, η, ϕ) is

$$ {}_0p = \frac{1}{c}(\cosh\eta - \mu)^{\frac{1}{2}} \sum_{m=0}^{\infty} \sum_{n=m}^{\infty} [A_n^m \sinh(n+\tfrac{1}{2})\eta + B_n^m \cosh(n+\tfrac{1}{2})\eta] \times \cosh(m\phi + \alpha_m) P_n^m(\mu), \tag{3.1} $$

$$ {}_0v_1 = \tfrac{1}{2}x_1\, {}_0p + \tfrac{1}{2}(u_0 + v_0)\cos(\phi + \alpha_0) + \tfrac{1}{2}(u_0 - v_0)\cos(\phi - \alpha_0) + \frac{1}{2}\sum_{m=1}^{\infty} \gamma_m \cos[(m+1)\phi + \alpha_m] + \frac{1}{2}\sum_{m=1}^{\infty} \chi_m \cos[(m-1)\phi + \alpha_m], \tag{3.2} $$

$$ {}_0v_2 = \tfrac{1}{2}x_2\, {}_0p + \tfrac{1}{2}(u_0 + v_0)\sin(\phi + \alpha_0) + \tfrac{1}{2}(u_0 - v_0)\sin(\phi - \alpha_0) + \frac{1}{2}\sum_{m=1}^{\infty} \gamma_m \sin[(m+1)\phi + \alpha_m] + \frac{1}{2}\sum_{m=1}^{\infty} \chi_m \sin[(m-1)\phi + \alpha_m], \tag{3.3} $$

$$ {}_0v_3 = \tfrac{1}{2}x_3\, {}_0p + (\cosh\eta - \mu)^{\frac{1}{2}} \sum_{m=0}^{\infty} \sum_{n=m}^{\infty} C_n^m \sinh(n+\tfrac{1}{2})\eta \cos(m\phi + \alpha_m) P_n^m(\mu), \tag{3.4} $$

where the α_m ($m = 0, 1, 2, \ldots$) are constant phase angles, and

$$ \gamma_m = (\cosh\eta - \mu)^{\frac{1}{2}} \sum_{n=m+1}^{\infty} [D_n^m \sinh(n+\tfrac{1}{2})\eta + E_n^m \cosh(n+\tfrac{1}{2})\eta] P_n^{m+1}(\mu), \tag{3.5a} $$

$$ \chi_m = (\cosh\eta - \mu)^{\frac{1}{2}} \sum_{n=m-1}^{\infty} [F_n^m \sinh(n+\tfrac{1}{2})\eta + G_n^m \cosh(n+\tfrac{1}{2})\eta] P_n^{m-1}(\mu), \tag{3.5b} $$

$$ u_0 = (\cosh\eta - \mu)^{\frac{1}{2}} \sum_{n=0}^{\infty} [D_n^0 \sinh(n+\tfrac{1}{2})\eta + E_n^0 \cosh(n+\tfrac{1}{2})\eta] P_n^1(\mu), \tag{3.5c} $$

$$ v_0 = (\cosh\eta - \mu)^{\frac{1}{2}} \sum_{n=0}^{\infty} [F_n^0 \sinh(n+\tfrac{1}{2})\eta + G_n^0 \cosh(n+\tfrac{1}{2})\eta] P_n^1(\mu). \tag{3.5d} $$

Here, $\mu = \cos\xi$, while the coordinate systems (x_1, x_2, x_3), (r_1, ϕ, x_3) and (ξ, η, ϕ) are interrelated by the equations:

$$x_1 = r_1\cos\phi, \quad x_2 = r_1\sin\phi, \quad x_3 = c\sinh\eta(\cosh\eta-\mu)^{-1},$$

in which

$$r_1 = c(1-\mu^2)^{\frac{1}{2}}(\cosh\eta-\mu)^{-1}.$$

P_n^m is the associated Legendre function of the first kind.

In the (ξ, η, ϕ) system the plane $x_3 = 0$ and the sphere surface respectively correspond to $\eta = 0$ and $\eta = \cosh^{-1}(\kappa^{-1})$ or, equivalently, $\eta = \coth^{-1}(1/\kappa c)$.

In order to satisfy the continuity equation (2.15*b*) and the no-slip wall boundary condition (2.17), the following relations must exist between $A_n^m, B_n^m, \ldots, G_n^m$:†

For $m = 0$,

$$-\tfrac{1}{2}nA_{n-1}^0+\tfrac{5}{2}A_n^0+\tfrac{1}{2}(n+1)A_{n+1}^0-n(n-1)D_{n-1}^0+2n(n+1)D_n^0-(n+1)(n+2)D_{n+1}^0 = 0 \tag{3.6}$$

and

$$-\tfrac{1}{2}nB_{n-1}^0+\tfrac{5}{2}B_n^0+\tfrac{1}{2}(n+1)B_{n+1}^0-nC_{n-1}^0+(2n+1)C_n^0-(n+1)C_{n+1}^0$$
$$-n(n-1)E_{n-1}^0+2n(n+1)E_n^0-(n+1)(n+2)E_{n+1}^0 = 0; \tag{3.7}$$

For $m \geqslant 1$,

$$-\tfrac{1}{2}(n-m)\{A_{n-1}^m; B_{n-1}^m\}+\tfrac{5}{2}\{A_n^m; B_n^m\}+\tfrac{1}{2}(n+m+1)\{A_{n+1}^m; B_{n+1}^m\}-(n-m)\{0; C_{n-1}^m\}$$
$$+(2n+1)\{0; C_n^m\}-(n+m+1)\{0; C_{n+1}^m\}-\tfrac{1}{2}(n-m)(n-m-1)\{D_{n-1}^m; E_{n-1}^m\}$$
$$+(n-m)(n+m+1)\{D_n^m; E_n^m\}-\tfrac{1}{2}(n+m+1)(n+m+2)\{D_{n+1}^m; E_{n+1}^m\}-\tfrac{1}{2}\{F_{n-1}^m; G_{n-1}^m\}$$
$$+\{F_n^m; G_n^m\}-\tfrac{1}{2}\{F_{n+1}^m; G_{n+1}^m\} = 0; \tag{3.8; 3.9}$$

For all m,

$$-\frac{(n-m-1)}{2n-1}E_{n-1}^m+E_n^m-\frac{(n+m+2)}{2n+3}E_{n+1}^m = -\frac{1}{2}\left[\frac{B_{n-1}^m}{2n-1}-\frac{B_{n+1}^m}{2n+3}\right]; \tag{3.10*a*}$$

For $m \geqslant 0$,

$$-\frac{(n-m+1)}{2n-1}G_{n-1}^m+G_n^m-\frac{n+m}{2n+3}G_{n+1}^m$$
$$= -\frac{1}{2}\left[-\frac{(n-m)(n-m+1)}{2n-1}B_{n-1}^m+\frac{(n+m)(n+m+1)}{2n+3}B_{n+1}^m\right] = 0; \tag{3.10*b*}$$

For $m = 0$,

$$G_n^0 = 0. \tag{3.10*c*}$$

The unique solution of the differential equations (2.15) and boundary conditions (2.16)–(2.18) is obtained by requiring that (3.1)–(3.4) satisfy the conditions

$${}_0v_i = U_i+\epsilon_{ijk}\Omega_j\bar{x}_k \quad \text{on } \eta = \eta_o \equiv \cosh^{-1}(\kappa^{-1}). \tag{3.11}$$

† In (3.6)–(3.9), algebraic sign errors contained in the comparable equations (3.3)–(3.5) of Lee & Leal (1980) have been corrected.

Towards satisfaction of this condition it is convenient to express the fluid velocity distribution on the sphere in the expanded form

$$
\begin{aligned}
{}_0v_1 = \tfrac{1}{2}(\cosh\eta_o-\mu)^{\frac{1}{2}}\Bigg\{ & \sum_{n=1}^{\infty}[X_n^0(\eta_o)+Y_n^0(\eta_o)]\cos(\phi+\alpha_0)P_n^1(\mu) \\
& + \sum_{n=1}^{\infty}[X_n^0(\eta_o)-Y_n^0(\eta_o)]\cos(\phi-\alpha_0)P_n^1(\mu) + \sum_{m=1}^{\infty}\sum_{n=m+1}^{\infty}X_n^m(\eta_o)\cos[(m+1)\phi+\alpha_m] \\
& \times P_n^{m+1}(\mu) + \sum_{m=1}^{\infty}\sum_{n=m-1}^{\infty}Y_n^m(\eta_o)\cos[(m-1)\phi+\alpha_m]P_n^{m-1}(\mu)\Bigg\},
\end{aligned}
\tag{3.12}
$$

$$
\begin{aligned}
{}_0v_2 = \tfrac{1}{2}(\cosh\eta_o-\mu)^{\frac{1}{2}}\Bigg\{ & \sum_{n=1}^{\infty}[X_n^0(\eta_o)+Y_n^0(\eta_o)]\sin(\phi+\alpha_0)P_n^1(\mu) \\
& + \sum_{n=1}^{\infty}[X_n^0(\eta_o)-Y_n^0(\eta_o)]\sin(\phi-\alpha_0)P_n^1(\mu) + \sum_{m=1}^{\infty}\sum_{n=m+1}^{\infty}X_n^m(\eta_o)\sin[(m+1)\phi+\alpha_m] \\
& \times P_n^{m+1}(\mu) + \sum_{m=1}^{\infty}\sum_{n=m-1}^{\infty}Y_n^m(\eta_o)\sin[(m-1)\phi+\alpha_m]P_n^{m-1}(\mu)\Bigg\},
\end{aligned}
\tag{3.13}
$$

$$
{}_0v_3 = (\cosh\eta_o-\mu)^{\frac{1}{2}}\sum_{m=0}^{\infty}\sum_{n=m}^{\infty}Z_n^m(\eta_o)\cos(m\phi+\alpha_m)P_n^m(\mu). \tag{3.14}
$$

Satisfaction of (3.11) requires that the three pairs of coefficients $\{X_n^m;\alpha_m\}$, $\{Y_n^m;\alpha_m\}$ and $\{Z_n^m;\alpha_m\}$ be given by

$$
X_n^m = 0 \quad \text{for all } m \text{ and } n, \tag{3.15a}
$$

$$
\{Y_n^0;\alpha_0\} = \{2\sqrt{2c}\exp[-(n+\tfrac{1}{2})\eta_o]\Omega_3;0\}, \tag{3.15b}
$$

$$
\begin{aligned}
\{Y_n^1;\alpha_1\} = {} & \{2\sqrt{2c}\exp[-(n+\tfrac{1}{2})\eta_o][U_1-\Omega_2(2n+1+\coth\eta_o)];0\} \\
& +\{2\sqrt{2c}\exp[-(n+\tfrac{1}{2})\eta_o][U_2-\Omega_1(2n+1+\coth\eta_o)];\tfrac{1}{2}\pi\},
\end{aligned}
\tag{3.15c}
$$

$$
\{Z_n^0;\alpha_0\} = \{\sqrt{2c}\exp[-(n+\tfrac{1}{2})\eta_o]U_3;0\}, \tag{3.15d}
$$

$$
\{Z_n^1;\alpha_1\} = \{-2\sqrt{2c}\exp[-(n+\tfrac{1}{2})\eta_o]\Omega_2;0\}+\{-2\sqrt{2c}\exp[-(n+\tfrac{1}{2})\eta_o]\Omega_1;\tfrac{1}{2}\pi\}. \tag{3.15e}
$$

All remaining coefficients Y_n^m and Z_n^m, i.e. those that do not explicitly appear in (3.15), are zero-valued in the expansion of (3.11).

Upon evaluating (3.2)–(3.4) at $\eta = \eta_o$, and comparing the resulting expressions with (3.12)–(3.14), we arrive at the following relations between $A_n^m, B_n^m, \ldots, G_n^m$ on the one hand, and X_n^m, Y_n^m and Z_n^m on the other:

$$
\begin{aligned}
D_n^m\sinh(n+\tfrac{1}{2})\eta_o + E_n^m\cosh(n+\tfrac{1}{2})\eta_o = {} & X_n^m(\eta_o) - \frac{1}{(2n+3)\sinh\eta_o}[-Z_{n+1}^m(\eta_o) \\
& + C_{n+1}^m\sinh(n+\tfrac{3}{2})\eta_o] + \frac{1}{(2n-1)\sinh\eta_o}[-Z_{n-1}^m(\eta_o)+C_{n-1}^m\sinh(n-\tfrac{1}{2})\eta_o] \quad \text{for all } m,
\end{aligned}
\tag{3.16}
$$

$$
G_n^0\cosh(n+\tfrac{1}{2})\eta_o + F_n^0\sinh(n+\tfrac{1}{2})\eta_o = Y_n^0(\eta_o), \tag{3.17a}
$$

$$G_n^m \cosh(n+\tfrac{1}{2})\eta_o + F_n^m \sinh(n+\tfrac{1}{2})\eta_o$$
$$= \frac{(n+m)(n+m+1)}{(2n+3)\sinh\eta_o}[-Z_{n+1}^m(\eta_o) + C_{n+1}^m \sinh(n+\tfrac{3}{2})\eta_0]$$
$$-\frac{(n-m)(n-m+1)}{(2n-1)\sinh\eta_o}[-Z_{n-1}^m(\eta_o) + C_{n-1}^m \sinh(n-\tfrac{1}{2})\eta_o] \quad \text{for } m \geqslant 1, \quad (3.17b)$$

$$A_n^m \sinh(n+\tfrac{1}{2})\eta_o + B_n^m \cosh(n+\tfrac{1}{2})\eta_o = -\frac{2}{\sinh\eta_o}$$
$$\times\left\{\frac{(n-m)}{2n-1}[Z_{n-1}^m(\eta_o) - C_{n-1}^m \sinh(n-\tfrac{1}{2})\eta_o] - \cosh\eta_o[Z_n^m(\eta_o) - C_n^m \sinh(n+\tfrac{1}{2})\eta_o]\right.$$
$$\left.+\frac{n+m+1}{2n+3}[Z_{n+1}^m(\eta_o) - C_{n+1}^m \sinh(n+\tfrac{3}{2})\eta_o]\right\} \quad \text{for all } m. \quad (3.18)$$

3.2. *First-order solution*

Define the ancillary fields $({}_1v_i^*, {}_1p^*)$ and $({}_1\hat{v}_i, {}_1\hat{p})$ by the expressions

$${}_1v_i = {}_1v_i^* + {}_1\hat{v}_i, \quad {}_1p = {}_1p^* + {}_1\hat{p}. \quad (3.19a,b)$$

The field $({}_1v_i^*, {}_1p^*)$ satisfies (2.19), (2.21) and (2.22), whilst the field $({}_1\hat{v}_i, {}_1\hat{p})$ satisfies, in addition to (2.19) and (2.22), the no-slip boundary condition

$${}_1\hat{v}_i = 0 \quad \text{on } x_3 = 0, \quad (3.20)$$

as well as the condition

$${}_1\hat{v}_i = -{}_1v_i^* \quad \text{on } x_1^2 + x_2^2 + (x_3 - \kappa^{-1})^2 = 1. \quad (3.21)$$

3.2.1. *The field* $({}_1v_i^*, {}_1p^*)$

Explicit determination of the wall boundary condition satisfied by $({}_1v_i^*, {}_1p^*)$ on $x_3 = 0$ necessitates calculation of ${}_0v_{i,3}$ at $x_3 = 0$. From the identity (cf. Dean & O'Neill 1963)

$$\left\{\frac{\partial}{\partial x_3}[(\cosh\eta - \mu)^{\frac{1}{2}} f(\eta)\, g(\xi)]\right\}_{x_3=0} = c^{-1}(1-\mu)^{\frac{3}{2}}\left[\frac{\mathrm{d}f}{\mathrm{d}\eta}\right]_{\eta=0} g(\xi), \quad (3.22)$$

and the recurrence formula

$$\mu P_n^m = (2n+1)^{-1}[(n-m+1)P_{n+1}^m + (n+m)P_{n-1}^m], \quad (3.23)$$

it can be deduced that on $\eta = 0$,

$${}_0v_{1,3} = \frac{1}{2c}(1-\mu)^{\frac{1}{2}}\left\{\frac{r_1}{c}\cos\phi \sum_{m=0}^{\infty}\sum_{n=m}^{\infty} H_n^m P_n^m(\mu)\cos(m\phi+\alpha_m) + \frac{1}{2}\left[\sum_{n=1}^{\infty} \bar{J}_n^0 P_n^1(\mu)\cos(\phi+\alpha_0)\right.\right.$$
$$\left.\left.+\sum_{n=1}^{\infty} \bar{K}_n^0 P_n^1(\mu)\cos(\phi-\alpha_0) + \sum_{m=0}^{\infty}\sum_{n=m}^{\infty} J_n^m P_n^m(\mu)\cos(m\phi+\alpha_m)\right]\right\}, \quad (3.24a)$$

$${}_0v_{2,3} = \frac{1}{2c}(1-\mu)^{\frac{1}{2}}\left\{\frac{r_1}{c}\sin\phi \sum_{m=0}^{\infty}\sum_{n=m}^{\infty} H_n^m P_n^m(\mu)\cos(m\phi+\alpha_m)\right.$$
$$+\frac{1}{2}\left[\sum_{n=1}^{\infty} \bar{J}_n^0 P_n^1(\mu)\sin(\phi+\alpha_0) + \sum_{n=1}^{\infty} \bar{K}_n^0 P_n^1(\mu)\sin(\phi-\alpha_0)\right.$$
$$\left.\left.+\sum_{m=0}^{\infty}\sum_{n=m}^{\infty} J_n^m P_n^m(\mu)\sin(m\phi+\alpha_m)\right]\right\}, \quad (3.24b)$$

and

$${}_0v_{3,3} = 0. \quad (3.24c)$$

Here, $$H_n^m = T(A_n^m) \overset{\text{def}}{\equiv} (n+\tfrac{1}{2})A_n^m - \tfrac{1}{2}(n-m)A_{n-1}^m - \tfrac{1}{2}(n+m+1)A_{n+1}^m, \tag{3.25a}$$

$$J_n^m = (1-\delta_{m0}-\delta_{m1})[(n+\tfrac{1}{2})D_n^{m-1} - \tfrac{1}{2}(n-m)D_{n-1}^{m-1} - \tfrac{1}{2}(n+m+1)D_{n+1}^{m-1}] + (n+\tfrac{1}{2})F_n^{m+1} - \tfrac{1}{2}(n-m)F_{n-1}^{m+1} - \tfrac{1}{2}(n+m+1)F_{n+1}^{m+1}, \tag{3.25b}$$

$$\bar{J}_n^0 = T(D_n^0 + F_n^0), \quad \bar{K}_n^0 = T(D_n^0 - F_n^0). \tag{3.25c,d}$$

For later reference it will prove convenient to define harmonic functions ϕ_0, ϕ_1 and ϕ_2 (containing the preceding constants) as

$$\phi_0 = \frac{1}{c^2}(\cosh\eta - \mu)^{\frac{1}{2}} \sum_{m=0}^{\infty} \sum_{n=m}^{\infty} H_n^m P_n^m(\mu) \cos(m\phi + \alpha_m) \exp[-(n+\tfrac{1}{2})\eta], \tag{3.26a}$$

$$\phi_1 = \frac{1}{2c}(\cosh\eta - \mu)^{\frac{1}{2}} \Bigg\{ \sum_{n=1}^{\infty} \bar{J}_n^0 P_n^1(\mu) \cos(\phi + \alpha_0) \exp[-(n+\tfrac{1}{2})\eta] + \sum_{n=1}^{\infty} \bar{K}_n^0 P_n^1(\mu) \cos(\phi - \alpha_0) \exp[-(n+\tfrac{1}{2})\eta] + \sum_{m=0}^{\infty} \sum_{n=m}^{\infty} J_n^m P_n^m(\mu) \cos(m\phi + \alpha_m) \times \exp[-(n+\tfrac{1}{2})\eta] \Bigg\}, \tag{3.26b}$$

$$\phi_2 = \frac{1}{2c}(\cosh\eta - \mu)^{\frac{1}{2}} \Bigg\{ \sum_{n=1}^{\infty} \bar{J}_n^0 P_n^1(\mu) \sin(\phi + \alpha_0) \exp[-(n+\tfrac{1}{2})\eta] + \sum_{n=1}^{\infty} \bar{K}_n^0 P_n^1(\mu) \sin(\phi - \alpha_0) \exp[-(n+\tfrac{1}{2})\eta] + \sum_{m=0}^{\infty} \sum_{n=m}^{\infty} J_n^m P_n^m(\mu) \sin(m\phi + \alpha_m) \times \exp[-(n+\tfrac{1}{2})\eta] \Bigg\}. \tag{3.26c}$$

Note that these harmonic functions are nowhere singular in the region $\eta > 0$.

The field $({}_1v_i^*, {}_1p^*)$ is determined here by using a general solution of (2.1) and (2.2) in terms of harmonic functions (Falade & Brenner 1985; Aderogba 1977), invoking particular choices for these harmonic functions appropriate to satisfying the wall condition (2.21). The desired construction relies, *ab initio*, on the fact that if ψ_0 and ψ_i $(i = 1, 2, 3)$ are any harmonic functions, then

$${}_1v_i^* = \tfrac{1}{2}[(\psi_0 + x_k\psi_k)_{,i} - 2\psi_i] \tag{3.27a}$$

and

$${}_1p^* = \psi_{j,j} \tag{3.27b}$$

satisfy (2.19*a* and *b*). Passage from the general solution (3.27) to particular solutions appropriate for ${}_1v_i^*$ and ${}_1p^*$ is aided by the following results, all but the last of which are given by Falade & Brenner (1985) (in slightly different and less general versions): If $\boldsymbol{\Phi}(x_1, x_2, x_3)$ is harmonic in its domain of definition, so also are the functions

$$W_k(x_1, x_2, x_3; \boldsymbol{\Phi}) = x_k\boldsymbol{\Phi} - x_3 \int \boldsymbol{\Phi}_{,k}\, \mathrm{d}x_3, \tag{3.28a}$$

$$X_{jk}(x_1, x_2, x_3; \boldsymbol{\Phi}) = x_j W_k - x_3 \int W_{k,j}\, \mathrm{d}x_3, \tag{3.28b}$$

$$Y_{ijk}(x_1, x_2, x_3; \boldsymbol{\Phi}) = x_i X_{jk} - x_3 \int X_{jk,i}\, \mathrm{d}x_3, \tag{3.28c}$$

$$Z_{hijk}(x_1, x_2, x_3; \boldsymbol{\Phi}) = x_h Y_{ijk} - x_3 \int Y_{ijk,h}\, \mathrm{d}x_3 \tag{3.28d}$$

(with $h, i, j, k \neq 3$), provided that the integral functions† $\int \Phi \, dx_3$, $\int W_k \, dx_3$, $\int X_{jk} \, dx_3$ and $\int Y_{ijk} \, dx_3$ are themselves harmonic. The latter conditions are satisfied by the functions defined in (3.26), as is evidenced by the fact that if Φ is expressible in the form

$$\Phi = (\cosh\eta - \mu)^{\frac{1}{2}} \sum_{m=0}^{\infty} \sum_{n=m}^{\infty} a_n^m P_n^m(\mu) \cos(m\phi + \alpha_m) \begin{bmatrix} \sinh(n+\frac{1}{2})\eta \\ \cosh(n+\frac{1}{2})\eta \end{bmatrix}$$

then $\int \Phi \, dx_3$ may be expressed as

$$\int \Phi \, dx_3 = (\cosh\eta - \mu)^{\frac{1}{2}} \sum_{m=0}^{\infty} \sum_{n=m}^{\infty} b_n^m P_n^m(\mu) \cos(m\phi + \alpha_m) \begin{bmatrix} \cosh(n+\frac{1}{2})\eta \\ \sinh(n+\frac{1}{2})\eta \end{bmatrix}, \quad (3.29)$$

where the coefficients b_n^m are to be determined by solving‡ the infinite set of linear equations

$$a_n^m = -(n-m) b_{n-1}^m + (2n+1) b_n^m - (n+m+1) b_{n+1}^m. \quad (3.30)$$

To secure convergence of the infinite series in (3.29) it is required that

$$b_n^m \to 0 \quad \text{as } n \to \infty \quad \text{for all } m. \quad (3.31)$$

Guided by the fact that a necessary condition for (2.21) to be satisfied by ${}_1v_i^*$ is that

$${}_1v_i^* \sim \alpha_{km} x_m x_k {}_0v_{i,3} \quad \text{on } x_3 = 0,$$

we make the following choices for ψ_0 and ψ_i $(i = 1, 2, 3)$:

$$\psi_0 = -\tfrac{1}{4}\alpha_{ij}[Z_{ijkk}(x_1, x_2, x_3; \phi_0) + Y_{1ij}(x_1, x_2, x_3; \phi_1) + Y_{2ij}(x_1, x_2, x_3; \phi_2)], \quad (3.32)$$

$$\psi_1 = \tfrac{1}{4}\alpha_{ij}[Y_{1ij}(x_1, x_2, x_3; \phi_0) + X_{ij}(x_1, x_2, x_3; \phi_1)], \quad (3.33)$$

$$\psi_2 = \tfrac{1}{4}\alpha_{ij}[Y_{2ij}(x_1, x_2, x_3; \phi_0) + X_{ij}(x_1, x_2, x_3; \phi_2)], \quad (3.34)$$

in which $i, j, k = 1, 2$. In (3.32)–(3.34) the summation convention with respect to

† All explicit constants and functions of integration are to be omitted in the evaluation of

$$\int \Phi_{,k} \, dx_3, \quad \int W_{k,j} \, dx_3, \quad \int X_{jk,i} \, dx_3 \quad \text{and} \quad \int Y_{ijk,h} \, dx_3.$$

These integrals are, however, to be evaluated in accordance with (3.29)–(3.31).

‡ An algorithm for directly solving (3.30) subject to (3.31), without having to either invert a matrix or perform iterative calculations, has been developed. The algorithm involves evaluating the double sum

$$b_n^m = \sum_{n''=n}^{N} \left(\frac{\sum_{n'=m}^{n''} t_{n'}^m a_{n'}^m}{(n''+m+1) t_{n''}^m} \right)$$

for each m, where $t_{n'}^m = 0$ for $n' < m$, $t_m^m = 1$, $t_{m+1}^m = 2m+1$,

and $t_{n'}^m = (n'-m)^{-1}[(2n'-1) t_{n'-1}^m - (n'+m-1) t_{n'-2}^m]$ for $n' > m+1$.

The upper limit N is to be chosen sufficiently large such that $b_{N+1}^m \approx 0$.

repeated indices prevails. In the expression for ψ_3 that follows we omit the arguments (x_1, x_2, x_3) for the sake of brevity:

$$\psi_3 = \tfrac{1}{4}\alpha_{ij}\left\{\left[Y_{ijk}\left(\int\phi_{0,k}\,dx_3\right)+(2+\delta_{ij})X_{ij}\left(\int\phi_0\,dx_3\right)+2X_{ii}\left(\int^3\phi_{0,ij}\,dx_3\right)\right.\right.$$
$$+(1-\delta_{mn})\delta_{ij}X_{mn}\left(\int^3\phi_{0,mn}\,dx_3\right)+(4+\delta_{ij})W_j\left(\int^3\phi_{0,i}\,dx_3\right)$$
$$+(\delta_{ij}-\delta_{ik}\delta_{jk})W_k\left(\int^3\phi_{0,k}\,dx_3\right)$$
$$+3W_k\left(\int^5\phi_{0,ijk}\,dx_3\right)+3\int^5\phi_{0,ij}\,dx_3+\delta_{ij}\int^3\phi_0\,dx_3\Big]+\Big[X_{ij}\left(\int\phi_{k,k}\,dx_3\right)$$
$$+2W_i\left(\int\phi_j\,dx_3\right)+2W_i\left(\int^3\phi_{k,kj}\,dx_3\right)+(\delta_{ij}+2\delta_{ik}\delta_{jk})\int^3\phi_{k,k}\,dx_3$$
$$\left.\left.+2(1-\delta_{ij})\int^3\phi_{i,j}\,dx_3+3\int^5\phi_{k,kij}\,dx_3\right]\right\}, \tag{3.35}$$

in which $i,j,k,m,n = 1,2$. It has been tacitly assumed in writing (3.35) that $\alpha_{12} = \alpha_{21}$; otherwise, the resulting expression for ψ_3 would have been much lengthier. In (3.35), $\int^n(\,)\,dx_3$ denotes an n-tuple integral with respect to x_3, namely

$$\int^n(\,)\,dx_3 \overset{\text{def}}{\equiv} \underset{n\text{-times}}{\iint\cdots\int}(\,)\,dx_3\,dx_3\ldots dx_3.$$

However, our notation for the single integral ($n = 1$) retains its customary form, namely $\int(\,)\,dx_3$.

Inasmuch as the field $({}_1v_i^*, {}_1p^*)$ possesses no singularities in the domain presently occupied by the sphere, the forces and torques exerted on the sphere by this field are identically zero. With ψ_0 and ψ_i $(i = 1,2,3)$ now determined, ${}_1v_i^*$ and ${}_1p^*$ may be obtained by employing (3.27).

3.2.2. *The field* $({}_1\hat{v}_i, {}_1\hat{p})$

In order to determine the force and torque on the sphere to the first order in β it proves unnecessary to first calculate the field $({}_1\hat{v}_i, {}_1\hat{p})$. This is so because the Stokes force ${}_1F_i$ and torque ${}_1T_i$ arising from an arbitrary field satisfying (2.15) and (2.17), and which satisfies arbitrary velocity distributions v_{Sj} and $v_{\infty j}$ on the sphere and at infinity, respectively, are given by the expressions (Brenner 1964*b*; Goldman, Cox & Brenner 1967*b*)

$${}_1F_i = \int_S n_k P^{(t)}_{kij}(v_{Sj}-v_{\infty j})\,dS, \tag{3.36}$$

$${}_1T_i = \int_S n_k P^{(r)}_{kij}(v_{Sj}-v_{\infty j})\,dS. \tag{3.37}$$

Here, $P^{(t)}_{kij}$ and $P^{(r)}_{kij}$ derive their definitions from the respective relations

$$\sigma^{(t)}_{ij} = U_k P^{(t)}_{kij}, \quad \sigma^{(r)}_{ij} = \Omega_k P^{(r)}_{kij},$$

where $\sigma^{(t)}_{ij}$ is the stress tensor for the field $({}_0v_i, {}_0p)$ (equations (2.15)–(2.18)), corresponding to the case $\boldsymbol{\Omega} = \mathbf{0}$ in (2.16), whereas $\sigma^{(r)}_{ij}$ is the comparable stress tensor

corresponding to the case $\boldsymbol{U} = \boldsymbol{0}$ in (2.16); n_k is the unit outward-drawn normal vector to the surface S of the sphere over which (3.36) and (3.37) are to be evaluated; $\mathrm{d}S$ is a scalar element of surface area on the sphere.

Should it ever become necessary to calculate the force and torque on the sphere to order β^2, it would then be inevitable to calculate the field $({}_1\hat{v}_i, {}_1\hat{p})$, since the wall boundary condition (2.25) defining the second-order field requires explicit knowledge of ${}_1\hat{v}_i$. In principle, this first-order field may be determined by expanding $-{}_1v_i^*(\xi, \eta, \phi)$ in a series of the form (3.12)–(3.14). The resulting expansions, together with the general Stokes field (3.1)–(3.5), and appropriate equations which are equivalent to (3.6)–(3.10) and (3.15)–(3.18), may then be used to uniquely determine $({}_1\hat{v}_i, {}_1\hat{p})$. If expansions of the form (3.12)–(3.14) can be found for their respective auxiliary fields, terms of third and higher orders in the asymptotic expansions of the force and torque may also be calculated by employing the general procedure just outlined above. Though straightforward in principle, the length and tedium of the requisite algebraic calculations are daunting. Consequently, the scope of the present paper will not extend beyond calculating first-order curvature effects – explicitly, terms of order β in the asymptotic expansions of the force and torque for small β.

Observe that the first-order velocity field depends linearly upon the three independent wall curvature coefficients α_{ij} $(i,j = 1,2)$. However, as earlier noted, the dependence of the velocity field upon α_{12} (or α_{21}) may be eliminated by an appropriate choice of the coordinate axes. Therefore, by virtue of (3.36) and (3.37), the contribution of the first-order field to the sphere's hydrodynamic resistance also depends linearly upon the remaining non-zero coefficients, $\alpha_{11} \equiv \alpha_1$, say, and $\alpha_{22} \equiv \alpha_2$, say. Furthermore, it may be anticipated that the contribution of each of the ordered fields also depends upon the parameter κ (in addition to the principal values α_1 and α_2 of $\boldsymbol{\alpha}$), since this parameter features in all the ordered sets of differential equations and boundary conditions (2.15)–(2.26) governing each such field solution.

3.3. *Hydrodynamic resistivities*

Given the preceding remarks, we are led to conclude that when the sphere lies proximate to a mildly curved wall $(d/R_0 \ll 1)$ and when $\beta \ll 1$, the non-dimensional hydrodynamic force and torque (about the sphere centre)

$$F_i \overset{\text{def}}{=} \frac{F_i'}{6\pi\mu a}, \quad T_i \overset{\text{def}}{=} \frac{T_i'}{8\pi\mu a^2} \tag{3.38a,b}$$

exerted upon the translating–rotating sphere are

$$\boldsymbol{F} = {}_0\boldsymbol{F} + \beta\,{}_1\boldsymbol{F} + O(\beta^2), \quad \boldsymbol{T} = {}_0\boldsymbol{T} + \beta\,{}_1\boldsymbol{T} + O(\beta^2), \tag{3.39a,b}$$

where, for $n = 0, 1$,

$$-{}_n\boldsymbol{F} = {}_n\boldsymbol{K}^{\mathrm{t}} \cdot \boldsymbol{U} + \tfrac{4}{3}\,{}_n\boldsymbol{K}^{\mathrm{c}\P} \cdot \boldsymbol{\Omega}, \tag{3.40a}$$

$$-{}_n\boldsymbol{T} = {}_n\boldsymbol{K}^{\mathrm{c}} \cdot \boldsymbol{U} + {}_n\boldsymbol{K}^{\mathrm{r}} \cdot \boldsymbol{\Omega}. \tag{3.40b}$$

In these expressions ${}_n\boldsymbol{K}^{\mathrm{t}}$, ${}_n\boldsymbol{K}^{\mathrm{r}}$ and ${}_n\boldsymbol{K}^{\mathrm{c}}$ denote respective (dimensionless) translational, rotational and coupling Stokes hydrodynamic resistance dyadics for the sphere. (Here and throughout, the superscript ¶ denotes a transposed dyadic.) The resistance formulation (3.39) and (3.40) incorporates the usual (Brenner 1964*a*; Happel & Brenner 1965) kinetic symmetries of the hydrodynamic resistance dyadics for the

spherical particle in the presence of boundaries. This accounts for the presence of the same term ${}_n\boldsymbol{K}^{\mathrm{c}}$ in both (3.40*a*) and (3.40*b*).† This same reciprocity principle requires that ${}_n\boldsymbol{K}^{\mathrm{t}\P} = {}_n\boldsymbol{K}^{\mathrm{t}}$ and ${}_n\boldsymbol{K}^{\mathrm{r}\P} = {}_n\boldsymbol{K}^{\mathrm{r}}$. Moreover, the scalar and pseudoscalar resistance coefficients making up these resistance dyadics satisfy a variety of inequalities deriving from the positive-definiteness of the energy dissipation occurring within the fluid. Rather than tabulating the pertinent inequalities here explicitly, we shall instead simply note that the algebraic signs and numerical values subsequently obtained for these resistances are consistent with the requisite inequalities.

As the intrinsic resistance dyadics ${}_n\boldsymbol{K}^{()}$ are purely geometric in nature – dependent only upon the position (κ) of the sphere (centre) relative to the wall, and the respective $n = 0$ and $n = 1$ 'shapes' of the bounding wall in its proximity – we may employ geometric symmetry arguments (Brenner 1964*a*; Happel & Brenner 1965) to anticipate their general forms. These forms, subsequently tabulated in (3.44) and (3.47) for the respective $n = 0$ and $n = 1$ cases, have been confirmed to be consistent with the subsequent detailed numerics.

In the purely geometric context appropriate to discussing these dyadics, it proves convenient to rewrite the (non-dimensional) equation (2.13) of the wall W in the invariant form

$$\boldsymbol{i}_3 \cdot \boldsymbol{r} = \tfrac{1}{2}\beta \boldsymbol{r} \cdot \boldsymbol{\alpha} \cdot \boldsymbol{r} + O(\beta^2) \quad \text{on } W, \tag{3.41}$$

with $\boldsymbol{r} = \boldsymbol{i}_1 x_1 + \boldsymbol{i}_2 x_2 + \boldsymbol{i}_3 x_3$ the position vector drawn from the contact point Q, and $\boldsymbol{i}_k$ a unit vector in the x_k direction. In (3.41) we note that $\boldsymbol{\alpha} = \boldsymbol{\alpha}^{\P}$ and $\boldsymbol{i}_3 \cdot \boldsymbol{\alpha} = \boldsymbol{0}$. In terms of the principal axes of the curvature dyadic $\boldsymbol{\alpha} = \boldsymbol{i}_j \boldsymbol{i}_k \alpha_{jk}$ (summation convention) of W at Q, we have that

$$\boldsymbol{\alpha} = \boldsymbol{i}_1 \boldsymbol{i}_1 \alpha_1 + \boldsymbol{i}_2 \boldsymbol{i}_2 \alpha_2, \tag{3.42}$$

with (α_1, α_2) the principal curvatures, given explicitly by the expressions

$$\alpha_1 = \frac{\partial^2 f}{\partial x_1^2}, \quad \alpha_2 = \frac{\partial^2 f}{\partial x_2^2}. \tag{3.43a,b}$$

The orthonormal system of unit vectors will be supposed ordered so as to constitute a right-handed system in the natural order $(\boldsymbol{i}_1, \boldsymbol{i}_2, \boldsymbol{i}_3)$.

As a consequence of (3.41), the geometric shape of the combined sphere/curved-wall configuration is governed to $O(\beta)$ by the directional parameters $\boldsymbol{i}_3$ and $\boldsymbol{\alpha}$.

3.3.1. *Zero-order resistivities* ${}_0\boldsymbol{K}^{()}(\boldsymbol{i}_3; \kappa)$

To terms of $O(\beta^0)$ in (3.41), the wall W is defined by the equation $\boldsymbol{i}_3 \cdot \boldsymbol{r} \equiv x_3 = 0$ on W. Thus, the $n = 0$ resistance coefficients in (3.39) correspond to the case of a sphere in proximity to a *plane* wall. With $\boldsymbol{i}_3$ normal to W (and pointing in a direction that passes through the sphere centre O; cf. figure 1), the geometric symmetry of the sphere/plane-wall configuration corresponds to that of transverse isotropy (i.e. the symmetry of a body of revolution) with respect to the $\boldsymbol{i}_3$ axis. For the true tensors

† In this context the appearance of the extraneous factor of $\frac{4}{3}$ multiplying ${}_n\boldsymbol{K}^{\mathrm{c}\P}$ in (3.40*a*) arises from the fact that the numerical factor of 6π in the normalization of (3.38*a*) differs from the comparable numerical factor of 8π employed in the normalization of (3.38*b*). The extraneous factor arises only in the normalized non-dimensional form, but not, of course, in the usual dimensional form.

κ^{-1}	a	b	c	d	e†
∞	$1+\frac{9}{16}\kappa$	$1+\frac{9}{8}\kappa$	$1+\frac{5}{16}\kappa^3$	$1+\frac{1}{8}\kappa^3$	$\frac{1}{8}\kappa^4$
10	1.0595	1.1262	1.0003	1.0001	0.9012 (−5)
5	1.1259	1.2851	1.0025	1.0010	0.1385 (−3)
3	1.2272	1.5692	1.0118	1.0047	0.1020 (−2)
2	1.3828	2.1255	1.0418	1.0159	0.50247 (−2)
1.8	1.4452	2.3988	1.0589	1.0220	0.7687 (−3)
1.6	1.5344	2.8489	1.0879	1.0318	0.12543 (−1)
1.5	1.6007	3.1792	1.1126	1.0391	0.17110 (−1)
1.4	1.6755	3.7356	1.1430	1.0489	0.22613 (−1)
1.2	1.9527	6.3409	1.2766	1.0832	0.49638 (−1)
1.1	2.2643	11.4592	1.4549	1.1171	0.88763 (−1)
1.075	2.3943	14.8443	1.5308	1.1296	0.10887
1.050	2.5997	21.5858	1.6690	1.1451	0.13844
1.025	2.9547	41.7222	1.9170	1.1658	0.18104
1.005	3.7863	202.0544	2.5056	1.2005	0.34192
$1+\Delta^{-1}$	$\frac{8}{15}\ln\Delta+0.9588$	$\Delta+O(\ln\Delta)$	$\frac{2}{5}\ln\Delta+0.3817$	$1.2021+O(\Delta^{-1})$	$\frac{1}{10}\ln\Delta-0.1895$

† The parenthetical number $(-n)$ following the entry represents the exponent of ten (10^{-n}) by which the entry must be multiplied. For example, for $\kappa^{-1}=5$ we have that $e=0.1385\times10^{-3}$.

TABLE 1. Zero-order curvature wall-effect coefficients. In tables 1 and 2 we have that $\kappa=a/d$ and $\Delta=a/(d-a)$, so that the two are related by the expression $\kappa^{-1}=1+\Delta^{-1}$. The values shown for the two asymptotic limits, $\kappa^{-1}\to\infty$ and $\kappa^{-1}\to1$, respectively, were derived by the methods discussed in the Appendix.

${}_0\boldsymbol{K}^{\mathrm{t}}$ and ${}_0\boldsymbol{K}^{\mathrm{r}}$ and pseudotensor ${}_0\boldsymbol{K}^{\mathrm{c}}$, this symmetry requires (Brenner 1964*a*; Happel & Brenner 1965) that

$$ {}_0\boldsymbol{K}^{\mathrm{t}} = (\boldsymbol{I}-\boldsymbol{i}_3\boldsymbol{i}_3)\,a+\boldsymbol{i}_3\boldsymbol{i}_3\,b, \tag{3.44a} $$

$$ {}_0\boldsymbol{K}^{\mathrm{r}} = (\boldsymbol{I}-\boldsymbol{i}_3\boldsymbol{i}_3)\,c+\boldsymbol{i}_3\boldsymbol{i}_3\,d, \tag{3.44b} $$

$$ {}_0\boldsymbol{K}^{\mathrm{c}} = \boldsymbol{\epsilon}\cdot\boldsymbol{i}_3\,e. \tag{3.44c} $$

The canonical forms (3.44) for these hydrodynamic resistivities may be written in more conventional 'matrix' forms by using the usual representation

$$ \boldsymbol{I}=\boldsymbol{i}_1\boldsymbol{i}_1+\boldsymbol{i}_2\boldsymbol{i}_2+\boldsymbol{i}_3\boldsymbol{i}_3 \tag{3.45a} $$

for the unit dyadic, and

$$ \boldsymbol{\epsilon}=\boldsymbol{i}_1\boldsymbol{i}_2\boldsymbol{i}_3-\boldsymbol{i}_1\boldsymbol{i}_3\boldsymbol{i}_2+\boldsymbol{i}_2\boldsymbol{i}_3\boldsymbol{i}_1-\boldsymbol{i}_2\boldsymbol{i}_1\boldsymbol{i}_3+\boldsymbol{i}_3\boldsymbol{i}_1\boldsymbol{i}_2-\boldsymbol{i}_3\boldsymbol{i}_2\boldsymbol{i}_1 \tag{3.45b} $$

for the unit alternating triadic.

Each of the five scalar resistance coefficients a,b,c,d,e appearing in (3.44) is a function only of κ. Numerical values giving their functional dependence upon κ are already available from the sphere/plane-wall analyses of Goldman *et al.* (1967*a*) and Lee & Leal (1980) (and linear semilogarithmic interpolations thereof at internodal points). For later reference these coefficients are tabulated in table 1.

3.3.2. *First-order resistivities* ${}_1\boldsymbol{K}^{()}(\boldsymbol{i}_3,\boldsymbol{\alpha};\kappa)$

Given the previous choice of axes 1 and 2 such as to coincide with the principal axes of curvature of W at Q, and given the geometric symmetry of the sphere, the point-group symmetry elements of the combined sphere/first-order-wall configuration correspond to the existence of two mutually perpendicular planes of

reflection symmetry, namely the (x_3, x_1)- and (x_2, x_3)-planes – as may also be seen by writing (3.41) in the principal axis form

$$x_3 = \tfrac{1}{2}\beta(\alpha_1 x_1^2 + \alpha_2 x_2^2) + O(\beta^2) \quad \text{on } W. \tag{3.46}$$

As the first-order resistance tensors ${}_1K_{ij}^{()}$ in (3.40) are intrinsic geometrical properties of this configuration, these tensors must display these same symmetry properties. Accordingly, using well-known (Brenner 1964*a*; Happel & Brenner 1965) symmetry results for second-rank tensors and pseudotensors possessing two mutually perpendicular planes of reflection symmetry, we are led to the following generic expressions for the three first-order resistance dyadics:

$${}_1\boldsymbol{K}^{\mathrm{t}} = \boldsymbol{i}_1\boldsymbol{i}_1\,{}_1K_{11}^{\mathrm{t}} + \boldsymbol{i}_2\boldsymbol{i}_2\,{}_1K_{22}^{\mathrm{t}} + \boldsymbol{i}_3\boldsymbol{i}_3\,{}_1K_{33}^{\mathrm{t}}, \tag{3.47a}$$

$${}_1\boldsymbol{K}^{\mathrm{r}} = \boldsymbol{i}_1\boldsymbol{i}_1\,{}_1K_{11}^{\mathrm{r}} + \boldsymbol{i}_2\boldsymbol{i}_2\,{}_1K_{22}^{\mathrm{r}} + \boldsymbol{i}_3\boldsymbol{i}_3\,{}_1K_{33}^{\mathrm{r}}, \tag{3.47b}$$

$${}_1\boldsymbol{K}^{\mathrm{c}} = \boldsymbol{i}_1\boldsymbol{i}_2\,{}_1K_{12}^{\mathrm{c}} + \boldsymbol{i}_2\boldsymbol{i}_1\,{}_1K_{21}^{\mathrm{c}}, \tag{3.47c}$$

involving the six non-zero scalars ${}_1K_{ij}^{\mathrm{t}}$ and ${}_1K_{ij}^{\mathrm{r}}$ in addition to the two non-zero pseudoscalars ${}_1K_{ij}^{\mathrm{c}}$. Each of these eight coefficients depends upon κ, α_1 and α_2.

Now, the *linear* nature of the differential equations and boundary conditions (2.19)–(2.22) defining the first-order velocity and pressure fields $({}_1\boldsymbol{v}, {}_1p)$ – the latter fields leading eventually to the first-order forces and torques $({}_1\boldsymbol{F}, {}_1\boldsymbol{T})$, and hence ultimately to the first-order resistance dyadics ${}_1\boldsymbol{K}^{()}$ – is such as to render these resistance tensors *linearly* dependent upon the α_{ij}.† Accordingly, in terms of the principal values α_1 and α_2 of α_{ij}, each of the eight resistance coefficients appearing in (3.47) must be expressible as the *linear* combination

$${}_1K_{ij}^{()} = \alpha_1\,{}^{[1]}_{1}K_{ij}^{()} + \alpha_2\,{}^{[2]}_{1}K_{ij}^{()}, \tag{3.48}$$

wherein each of the coefficients ${}^{[\,]}_{1}K_{ij}^{()}$ appearing on the right-hand side of (3.48) depends only upon κ. In particular, these coefficients are independent of α_1 and α_2.

The expression (3.42) and (3.43) remains invariant, of course, under a positive 90° rotation about the x_3 axis. This rotation effects the index label changes $1 \to -2$ and $2 \to 1$, corresponding to the formal interchange of α_1 with α_2 (as well as $\boldsymbol{i}_1$ with $-\boldsymbol{i}_2$ and $\boldsymbol{i}_2$ with $\boldsymbol{i}_1$). It readily follows that for the true scalar resistance coefficients we must have that

$${}^{[1]}_{1}K_{11}^{\mathrm{t}} = {}^{[2]}_{1}K_{22}^{\mathrm{t}} \equiv A, \quad {}^{[2]}_{1}K_{11}^{\mathrm{t}} = {}^{[1]}_{1}K_{22}^{\mathrm{t}} \equiv B, \quad {}^{[1]}_{1}K_{33}^{\mathrm{t}} = {}^{[2]}_{1}K_{33}^{\mathrm{t}} \equiv C, \tag{3.49a,b,c}$$

† Explicitly, since the only inhomogeneous term appearing in the system of equations defining $({}_1v_i, {}_1p)$ arises on the right-hand side of (2.21), it becomes possible to determine a (tensorially) third-rank 'velocity' field ${}_1V_{ikm}$ and second-order 'pressure' field ${}_1P_{km}$, respectively defined via the relations

$${}_1v_i = {}_1V_{ikm}\,\alpha_{km}, \quad {}_1p = {}_1P_{km}\,\alpha_{km}.$$

From (2.19)–(2.22) this pair of Cartesian tensor fields satisfies the system of equations

$${}_1V_{ikm,jj} - {}_1P_{km,i} = 0, \quad {}_1V_{jkm,j} = 0,$$

$${}_1V_{ikm} = 0 \quad \text{on } x_1^2 + x_2^2 + (x_3 - \kappa^{-1})^2 = 1,$$

$${}_1V_{ikm} = -\tfrac{1}{2}x_k x_m\,{}_0v_{i,3} \quad \text{on } x_3 = 0,$$

$${}_1V_{ijm,3} \to 0 \quad \text{as } |r| \to \infty.$$

As this system of defining equations is independent of the curvature dyadic $\boldsymbol{\alpha}$, one can (in principle) imagine first solving these for ${}_1V_{ikm}(\kappa)$ and ${}_1P_{km}(\kappa)$, subsequently deriving therefrom the original fields ${}_1v_i(\kappa;\boldsymbol{\alpha})$ and ${}_1p(\kappa;\boldsymbol{\alpha})$ via the preceding pair of *linear* $\boldsymbol{\alpha}$ transformations. This scheme makes evident the explicit linear $\boldsymbol{\alpha}$ dependence displayed in (3.48).

say, for translation, and

$$ {}^{[1]}_{1}K^{\mathrm{r}}_{11} = {}^{[2]}_{1}K^{\mathrm{r}}_{22} \equiv D, \quad {}^{[2]}_{1}K^{\mathrm{r}}_{11} = {}^{[2]}_{1}K^{\mathrm{r}}_{22} \equiv E, \quad {}^{[1]}_{1}K^{\mathrm{r}}_{33} = {}^{[2]}_{1}K^{\mathrm{r}}_{33} \equiv F, \quad (3.50a,b,c) $$

say, for rotation. On the other hand, for the pseudoscalar resistance coefficients we require that

$$ {}^{[1]}_{1}K^{\mathrm{c}}_{12} = -{}^{[2]}_{1}K^{\mathrm{c}}_{21} \equiv -G, \quad {}^{[1]}_{1}K^{\mathrm{c}}_{21} = -{}^{[2]}_{1}K^{\mathrm{c}}_{12} \equiv H, \qquad (3.51a,b) $$

say, for the coupling case.

Consequently, in the principal axis system, $(\boldsymbol{i}_1, \boldsymbol{i}_2, \boldsymbol{i}_3)$, the first-order resistance dyadics can be written as

$$ {}_1\boldsymbol{K}^{\mathrm{t}} = \alpha_1(\boldsymbol{i}_1\boldsymbol{i}_1 A + \boldsymbol{i}_2\boldsymbol{i}_2 B + \boldsymbol{i}_3\boldsymbol{i}_3 C) + \alpha_2(\boldsymbol{i}_1\boldsymbol{i}_1 B + \boldsymbol{i}_2\boldsymbol{i}_2 A + \boldsymbol{i}_3\boldsymbol{i}_3 C), \qquad (3.52a) $$

$$ {}_1\boldsymbol{K}^{\mathrm{r}} = \alpha_1(\boldsymbol{i}_1\boldsymbol{i}_1 D + \boldsymbol{i}_2\boldsymbol{i}_2 E + \boldsymbol{i}_3\boldsymbol{i}_3 F) + \alpha_2(\boldsymbol{i}_1\boldsymbol{i}_1 E + \boldsymbol{i}_2\boldsymbol{i}_2 D + \boldsymbol{i}_3\boldsymbol{i}_3 F), \qquad (3.52b) $$

and

$$ {}_1\boldsymbol{K}^{\mathrm{c}} = -\alpha_1(\boldsymbol{i}_1\boldsymbol{i}_2 G - \boldsymbol{i}_2\boldsymbol{i}_1 H) - \alpha_2(\boldsymbol{i}_1\boldsymbol{i}_2 H - \boldsymbol{i}_2\boldsymbol{i}_1 G). \qquad (3.52c) $$

Equations (3.52) may be expressed in an invariant form, wholly in terms of the two fundamental directional parameters $\boldsymbol{i}_3$ and $\boldsymbol{\alpha}$ geometrically characterizing the first-order wall configuration (3.41), as

$$ {}_1\boldsymbol{K}^{\mathrm{t}} = \boldsymbol{\alpha}(A-B) + (\boldsymbol{I}:\boldsymbol{\alpha})[(\boldsymbol{I}-\boldsymbol{i}_3\boldsymbol{i}_3)B + \boldsymbol{i}_3\boldsymbol{i}_3 C], \qquad (3.53a) $$

$$ {}_1\boldsymbol{K}^{\mathrm{r}} = \boldsymbol{\alpha}(D-E) + (\boldsymbol{I}:\boldsymbol{\alpha})[(\boldsymbol{I}-\boldsymbol{i}_3\boldsymbol{i}_3)E + \boldsymbol{i}_3\boldsymbol{i}_3 F], \qquad (3.53b) $$

$$ {}_1\boldsymbol{K}^{\mathrm{c}} = -\boldsymbol{\alpha}\cdot(\boldsymbol{\epsilon}\cdot\boldsymbol{i}_3)G - (\boldsymbol{\epsilon}\cdot\boldsymbol{i}_3)\cdot\boldsymbol{\alpha}H. \qquad (3.53c) $$

The eight independent (true) scalar coefficients (A,B,C), (D,E,F) and (G,H) appearing in these canonically invariant expressions for the first-order resistance dyadics depend only upon κ. Numerical values of these coefficients *vs.* κ are tabulated in table 2, having been derived from the detailed computational scheme subsequently set forth in §4.

3.4. *Hydrodynamic forces and torques*

Substitution of the respective expressions (3.44) and (3.52) for the zeroth- and first-order resistance dyadics into the force and torque expressions (3.39) and (3.40) yields the following matrix relation for the non-dimensional force and torque on the sphere, correct to the first-order in β:

$$ -\begin{bmatrix} F_1 \\ F_2 \\ F_3 \\ T_1 \\ T_2 \\ T_3 \end{bmatrix} = \left[\begin{array}{ccc|ccc} a & \cdot & \cdot & \cdot & -\frac{4}{3}e & \cdot \\ \cdot & a & \cdot & \frac{4}{3}e & \cdot & \cdot \\ \cdot & \cdot & b & \cdot & \cdot & \cdot \\ \hline \cdot & e & \cdot & c & \cdot & \cdot \\ -e & \cdot & \cdot & \cdot & c & \cdot \\ \cdot & \cdot & \cdot & \cdot & \cdot & d \end{array}\right] \begin{bmatrix} U_1 \\ U_2 \\ U_3 \\ \Omega_1 \\ \Omega_2 \\ \Omega_3 \end{bmatrix} + \beta \left\{ \alpha_1 \left[\begin{array}{ccc|ccc} A & \cdot & \cdot & \cdot & \frac{4}{3}H & \cdot \\ \cdot & B & \cdot & -\frac{4}{3}G & \cdot & \cdot \\ \cdot & \cdot & C & \cdot & \cdot & \cdot \\ \hline \cdot & -G & \cdot & D & \cdot & \cdot \\ H & \cdot & \cdot & \cdot & E & \cdot \\ \cdot & \cdot & \cdot & \cdot & \cdot & F \end{array}\right] \right. $$

$$ \left. + \alpha_2 \left[\begin{array}{ccc|ccc} B & \cdot & \cdot & \cdot & \frac{4}{3}G & \cdot \\ \cdot & A & \cdot & -\frac{4}{3}H & \cdot & \cdot \\ \cdot & \cdot & C & \cdot & \cdot & \cdot \\ \hline \cdot & -H & \cdot & E & \cdot & \cdot \\ G & \cdot & \cdot & \cdot & D & \cdot \\ \cdot & \cdot & \cdot & \cdot & \cdot & F \end{array}\right] \right\} \begin{bmatrix} U_1 \\ U_2 \\ U_3 \\ \Omega_1 \\ \Omega_2 \\ \Omega_3 \end{bmatrix} + O(\beta^2). \qquad (3.54) $$

κ^{-1}	A	B	C	D	E	F	G	H
∞	81/128	27/128	9/32	0	0	0	$(27/128)\kappa$	$(9/128)\kappa$
10	0.6328	0.2109	0.2813	0.00000	0.00000	0.00000	0.02109	0.00704
5	0.6328	0.2109	0.2825	0.00009	0.00010	0.0046	0.04218	0.01408
3	0.6387	0.2127	0.5299	0.00015	0.00045	0.0075	0.0706	0.02341
2	0.6459	0.2157	0.9256	0.00022	0.00068	0.01851	0.1083	0.03582
1.8	0.6519	0.2168	1.1248	0.00071	0.00217	0.02362	0.1182	0.03923
1.6	0.6692	0.2221	1.4633	0.00151	0.00457	0.03125	0.1257	0.04171
1.5	0.7259	0.2416	1.7121	0.00359	0.01068	0.03818	0.1463	0.04849
1.4	0.8315	0.2777	2.1643	0.00625	0.01875	0.04892	0.1727	0.05752
1.2	1.1088	0.3655	4.3329	0.01065	0.03161	0.08427	0.2825	0.09378
1.1	1.7063	0.5294	8.7625	0.04681	0.0652	0.09832	0.3433	0.11528
1.075	1.9244	0.6012	10.5738	0.07929	0.0764	0.10258	0.3942	0.1285
1.050	2.3989	0.7734	16.7718	0.1602	0.1027	0.11329	0.4698	0.1448
1.025	3.0522	1.0122	33.9452	0.3229	0.1343	0.12952	0.6782	0.1942
1.005	4.6195	1.5509	180.9235	0.7505	0.3473	0.1686	1.0903	0.4811
$1+\Delta^{-1}$	$\frac{74}{75}\ln\Delta-0.6131$	$\frac{26}{75}\ln\Delta-0.2876$	$\Delta-0.2001\Delta^{\frac{1}{2}}+1.5613\ln\Delta$	$\frac{13}{50}\ln\Delta-0.6283$	$\frac{7}{50}\ln\Delta-0.3951$	$0.17960-2.2232\Delta^{-1}$	$\frac{1}{100}\ln\Delta+1.0374$	$\frac{19}{100}\ln\Delta-0.5266$

TABLE 2. First-order wall-effect coefficients (see also caption to table 1). The error estimates given for the case $\kappa > 1$ derive from the 'lubrication'-theory analysis of Cox (1974). For the case of the C coefficient the $O(\Delta^{\frac{1}{2}})$ error estimate applies generally when $\alpha_1 \neq \alpha_2$. For the special spherical-wall case, where $\alpha_1 = \alpha_2$, the $O(\ln\Delta)$ error estimate obtains, in accord with the results of Cooley & O'Neill (1969*b*) (see (5.5*d*)).

Readers interested only in applications of (3.54) may proceed directly to §5, omitting the detailed scheme outlined in §4 whereby numerical values of the first-order wall-effect coefficients $A, B, \ldots, H$ required in (3.54) are calculated as functions of κ.

4. Calculation of the first-order curvature coefficients

In view of the linear dependence of the first-order curvature effects upon the α_{ij} values explicit in (3.54), we may calculate those effects respectively proportional to α_1 and α_2 separately, for which the other curvature coefficient is identically zero. The general results for any curved wall (for which, of course, the conditions $\beta \ll 1$ and $d/R_0 \ll 1$ are satisfied) may then be established by linear superposition of the two separate sets of effects. Because precisely the same resistance coefficients (namely $A, B, \ldots, H$) feature in the α_1 coefficient matrix of (3.54) as in the comparable α_2 matrix, it suffices to focus exclusively upon only the α_1 term, say, in order to derive the results for the more general case where the curvatures α_1 and α_2 are simultaneously non-zero. This has been done in what follows.

Moreover, also owing to the linearity of the differential equations and boundary conditions, the contributions of the first-order field to sphere resistance when the sphere performs an arbitrary translational and rotational motion may be derived by linearly superposing the separate resistances for the six independent cases, in each of which either the sphere's direction of translational motion or its axis of rotation is parallel to one of the three coordinate axes. For this reason, calculations of the sphere's resistance for each of these six fundamental cases are separately given in subsequent subsections.

More explicit expressions can be written down for the vectors $n_k P^{(t)}_{kij} v_{Sj}$ and $n_k P^{(r)}_{kij} v_{Sj}$ (in a quiescent medium $v_{\infty j} = 0$) which feature in (3.36) and (3.37). In the first-order calculations, $v_{Sj} = -{}_1v^*_j$. Therefore, we have that (cf. Lamb 1932)

$$n_k P^{(t)}_{kij} v_{Sj} = \left[\bar{x}_i p^{(t)}_j - R\frac{\partial u^{(t)}_{ij}}{\partial R} - \bar{x}_k \frac{\partial u^{(t)}_{kj}}{\partial x_i}\right]_1 v^*_j, \tag{4.1}$$

$$n_k P^{(r)}_{kij} v_{Sj} = \epsilon_{imn}\bar{x}_n \left[\bar{x}_m p^{(r)}_j - R\frac{\partial u^{(r)}_{mj}}{\partial R} - \bar{x}_k \frac{\partial u^{(r)}_{kj}}{\partial x_m}\right]_1 v^*_j. \tag{4.2}$$

In (4.1), $u^{(t)}_{kj}$ and $p^{(t)}_j$ are the fluid velocity and pressure fields which satisfy (2.15), (2.17), (2.18) and the boundary condition

$$u^{(t)}_{kj} = \delta_{kj} \quad \text{on the sphere.}$$

Similarly, $u^{(r)}_{kj}$ and $p^{(r)}_j$ satisfy (2.15), (2.17), (2.18) and the condition

$$u^{(r)}_{kj} = \epsilon_{kpq}\delta_{pj}\bar{x}_q \quad \text{on the sphere.}$$

In (4.1) and (4.2), R is the spherical polar coordinate defined by the expression

$$R^2 = x_1^2 + x_2^2 + \bar{x}_3^2.$$

It is possible to simplify (4.1) somewhat by employing the following lemma: If g is a field quantity that adopts a constant value on the surface S of a sphere, then

$$\left(\bar{x}_i \frac{\partial}{\partial \bar{x}_j} - \bar{x}_j \frac{\partial}{\partial \bar{x}_i}\right) g = 0 \quad (i,j = 1,2,3; \quad i \neq j) \tag{4.3}$$

at all points on S. This result is readily established by expressing the Cartesian differential operator $\bar{x}_i(\partial/\partial\bar{x}_j)-\bar{x}_j(\partial/\partial\bar{x}_i)$ in polar coordinates, and noting that the derivative of g with respect to each polar coordinate except R vanishes if g is constant on S. Upon using (4.3) together with continuity equation (2.15b) in (4.1), we thereby obtain

$$n_k P^{(t)}_{kij} v_{Sj} = \left[\bar{x}_i p^{(t)}_j - R\frac{\partial u^{(t)}_{ij}}{\partial R}\right]_1 v^*_j. \tag{4.4}$$

4.1. *Translation parallel to the x_1 axis*

This subsection addresses the boundary-value problem corresponding to the case where $U_1 \neq 0$, while, simultaneously, $U_2 = U_3 = \Omega_1 = \Omega_2 = \Omega_3 = 0$. (Moreover, for reasons discussed earlier in this section, we shall only address the case for which $\alpha_1 \neq 0$, while, simultaneously, $\alpha_2 = 0$.)

From results given by Lee & Leal (1980) we deduce the following expressions for $p^{(t)}_j$ and $u^{(t)}_{kj}$ $(k,j = 1,2,3)$:

$$p^{(t)}_1 = c^{-1}\cos\phi(\cosh\eta-\mu)^{\frac{1}{2}}\sum_{n=1}^{\infty}[A^{1(t)}_n \sinh(n+\tfrac{1}{2})\eta + B^{1(t)}_n \cosh(n+\tfrac{1}{2})\eta]P^1_n, \tag{4.5a}$$

$$u^{(t)}_{11} = \tfrac{1}{2}x_1 p^{(t)}_1 + \tfrac{1}{2}(\cosh\eta-\mu)^{\frac{1}{2}}\left\{\sum_{n=0}^{\infty}[F^{1(t)}_n \sinh(n+\tfrac{1}{2})\eta + G^{1(t)}_n \cosh(n+\tfrac{1}{2})\eta]P^0_n + \cos 2\phi\sum_{n=2}^{\infty}[D^{1(t)}_n \sinh(n+\tfrac{1}{2})\eta + E^{1(t)}_n \cosh(n+\tfrac{1}{2})\eta]P^2_n\right\}, \tag{4.5b}$$

$$u^{(t)}_{12} = \tfrac{1}{2}x_2 p^{(t)}_1 + \tfrac{1}{2}\sin 2\phi(\cosh\eta-\mu)^{\frac{1}{2}}\sum_{n=2}^{\infty}[D^{1(t)}_n \sinh(n+\tfrac{1}{2})\eta + E^{1(t)}_n \cosh(n+\tfrac{1}{2})\eta]P^2_n, \tag{4.5c}$$

$$u^{(t)}_{13} = \tfrac{1}{2}x_3 p^{(t)}_1 + \tfrac{1}{2}\cos\phi(\cosh\eta-\mu)^{\frac{1}{2}}\sum_{n=1}^{\infty} C^{1(t)}_n \sinh(n+\tfrac{1}{2})\eta P^1_n; \tag{4.5d}$$

$$p^{(t)}_2 = c^{-1}\sin\phi(\cosh\eta-\mu)^{\frac{1}{2}}\sum_{n=1}^{\infty}[A^{1(t)}_n \sinh(n+\tfrac{1}{2})\eta + B^{1(t)}_n \cosh(n+\tfrac{1}{2})\eta]P^1_n, \tag{4.6a}$$

$$u^{(t)}_{21} = \tfrac{1}{2}x_1 p^{(t)}_2 - \tfrac{1}{2}\sin 2\phi(\cosh\eta-\mu)^{\frac{1}{2}}\sum_{n=2}^{\infty}[D^{1(t)}_n \sinh(n+\tfrac{1}{2})\eta + E^{1(t)}_n \cosh(n+\tfrac{1}{2})\eta]P^2_n, \tag{4.6b}$$

$$u^{(t)}_{22} = \tfrac{1}{2}x_2 p^{(t)}_2 + \tfrac{1}{2}(\cosh\eta-\mu)^{\frac{1}{2}}\left\{\sum_{n=0}^{\infty}[F^{1(t)}_n \sinh(n+\tfrac{1}{2})\eta + G^{1(t)}_n \cosh(n+\tfrac{1}{2})\eta]P^0_n - \cos 2\phi\sum_{n=2}^{\infty}[D^{1(t)}_n \sinh(n+\tfrac{1}{2})\eta + E^{1(t)}_n \cosh(n+\tfrac{1}{2})\eta]P^2_n\right\}, \tag{4.6c}$$

$$u^{(t)}_{23} = \tfrac{1}{2}x_3 p^{(t)}_2 + \sin\phi(\cosh\eta-\mu)^{\frac{1}{2}}\sum_{n=1}^{\infty} C^{1(t)}_n \sinh(n+\tfrac{1}{2})\eta P^1_n; \tag{4.6d}$$

$$p^{(t)}_3 = c^{-1}(\cosh\eta-\mu)^{\frac{1}{2}}\sum_{n=0}^{\infty}[A^{0(t)}_n \sinh(n+\tfrac{1}{2})\eta + B^{0(t)}_n \cosh(n+\tfrac{1}{2})\eta]P^0_n, \tag{4.7a}$$

$$u^{(t)}_{31} = \tfrac{1}{2}x_1 p^{(t)}_3 + \cos\phi(\cosh\eta-\mu)^{\frac{1}{2}}\sum_{n=1}^{\infty}[D^{0(t)}_n \sinh(n+\tfrac{1}{2})\eta + E^{0(t)}_n \cosh(n+\tfrac{1}{2})\eta]P^1_n, \tag{4.7b}$$

$$u^{(t)}_{32} = \tfrac{1}{2}x_2 p^{(t)}_3 + \sin\phi(\cosh\eta-\mu)^{\frac{1}{2}}\sum_{n=1}^{\infty}[D^{0(t)}_n \sinh(n+\tfrac{1}{2})\eta + E^{0(t)}_n \cosh(n+\tfrac{1}{2})\eta]P^1_n, \tag{4.7c}$$

$$u^{(t)}_{33} = \tfrac{1}{2}x_3 p^{(t)}_3 + (\cosh\eta-\mu)^{\frac{1}{2}}\sum_{n=0}^{\infty} C^{0(t)}_n \sinh(n+\tfrac{1}{2})\eta P^0_n. \tag{4.7d}$$

The coefficients $\overset{(t)}{A}{}_n^m, \overset{(t)}{B}{}_n^m, \ldots, \overset{(t)}{G}{}_n^m$ $(m = 0, 1)$ appearing in (4.5)–(4.7) are to be obtained by solving appropriate combinations of equations (3.6)–(3.10) and (3.16)–(3.18).

For a sphere translating parallel to the x_1 axis:

$$\phi_0 = c^{-2} \cos\phi (\cosh\eta - \mu)^{\frac{1}{2}} \sum_{n=1}^{\infty} \overset{(t)}{H}{}_n^1 P_n^1 \exp[-(n+\tfrac{1}{2})\eta], \tag{4.8a}$$

$$\phi_1 = c^{-1} \cos 2\phi (\cosh\eta - \mu)^{\frac{1}{2}} \left\{ \sum_{n=0}^{\infty} \overset{(t)}{J}{}_n^1 P_n^0 \exp[-(n+\tfrac{1}{2})\eta] + \sum_{n=2}^{\infty} \overset{(t)}{K}{}_n^1 P_n^2 \exp[-(n+\tfrac{1}{2})\eta] \right\}, \tag{4.8b}$$

$$\phi_2 = c^{-1} \sin 2\phi (\cosh\eta - \mu)^{\frac{1}{2}} \sum_{n=2}^{\infty} \overset{(t)}{K}{}_n^1 P_n^2 \exp[-(n+\tfrac{1}{2})\eta]. \tag{4.8c}$$

To determine ${}_1v_i^*$, we substitute ϕ_0, ϕ_1 and ϕ_2 from (4.8) into (3.32)–(3.35) to first determine ψ_0 and ψ_i $(i = 1, 2, 3)$, which are then employed in (3.27*a*). Having defined all the terms in (3.36) and (3.37), we are now in a position to evaluate the surface integrals appearing in these equations, and hence to determine the first-order force ${}_1F_i$ and torque ${}_1T_i$ exerted by the fluid on the sphere. These calculations require the evaluation of integrals possessing the following forms (or reducible thereto):

$$I_1 = \int_{-1}^{1} (\cosh\eta_o - \mu)^{-n} P_l^m(\mu) P_k^m(\mu)\, d\mu, \tag{4.9a}$$

and

$$I_2 = \int_{-1}^{1} \mu (\cosh\eta_o - \mu)^{-n} P_l^m(\mu) P_k^m(\mu)\, d\mu, \tag{4.9b}$$

$(m = 0, 1; n \geqslant 1)$. Results given in Gradshteyn & Ryzhik (1980; pp. 796, 821) can be used to demonstrate that

$$I_1 = \frac{2(-1)^{n-1}}{(n-1)!} \frac{d^{n-1}}{dz^{n-1}} [P_l^m(z) Q_k^m(z)] \qquad (l \leqslant k), \tag{4.10}$$

$$I_2 = \frac{2(-1)^{n-1}}{(n-1)!} \frac{d^{n-1}}{dz^{n-1}} [z P_l^m(z) Q_k^m(z)] \qquad (l < k), \tag{4.11a}$$

$$I_2 = \frac{2(-1)^{n-1}}{(n-1)!} \frac{d^{n-1}}{dz^{n-1}} \left[z P_l^m(z) Q_k^m(z) - \frac{1}{2l+1} \right] \quad (l = k > 1), \tag{4.11b}$$

in which $z = \cosh\eta_o$. Moreover, Q_k^m is the associated Legendre function of the second kind.

Numerical evaluation of the non-zero first-order force and torque coefficients $-{}_1F_1/\beta\alpha\,{}_1U_1 \equiv A$ and $-{}_1T_2/\beta\alpha\,{}_1U_1 \equiv H$ appearing in (3.54) have been performed for a range of κ values. The results are displayed in table 2. Also tabulated are asymptotic expressions for the limiting cases $\kappa \to 0$ and $\kappa \to 1$, respectively extracted from the 'reflection' analysis of Falade & Brenner (1985) and the 'lubrication' analysis of Cox (1974) by the methods discussed in the Appendix.

4.2. *Translation parallel to the x_2 axis*

For this case, ϕ_0, ϕ_1 and ϕ_2 are defined by the relations

$$\phi_0 = c^{-2} \sin\phi(\cosh\eta-\mu)^{\frac{1}{2}} \sum_{n=1}^{\infty} {}^{(t)}H_n^1 P_n^1 \exp[-(n+\tfrac{1}{2})\eta], \tag{4.12a}$$

$$\phi_1 = -c^{-1} \sin 2\phi(\cosh\eta-\mu)^{\frac{1}{2}} \sum_{n=2}^{\infty} {}^{(t)}K_n^1 P_n^2 \exp[-(n+\tfrac{1}{2})\eta], \tag{4.12b}$$

$$\phi_2 = c^{-1} \cos 2\phi(\cosh\eta-\mu)^{\frac{1}{2}} \left\{ \sum_{n=0}^{\infty} {}^{(t)}J_n^1 P_n^0 \exp[-(n+\tfrac{1}{2})\eta] + \sum_{n=2}^{\infty} {}^{(t)}K_n^1 P_n^2 \exp[-(n+\tfrac{1}{2})\eta] \right\}. \tag{4.12c}$$

Equations (4.12) are used first in (3.32)–(3.35) and then in (3.27a) to determine ${}_1v_i^*$ for this case. The first-order curvature effects upon the force ${}_1F_i$ and torque ${}_1T_i$ are determined by evaluating the integrals in (3.36) and (3.37). The results of these calculations yield the non-zero first-order force and torque coefficients $-{}_1F_2/\beta\alpha\,{}_1U_2 \equiv B$ and $-{}_1T_1/\beta\alpha\,{}_1U_2 \equiv -G$ of (3.54). Numerical values of these two coefficients as a function of κ are given in table 2.

4.3. *Translation parallel to the x_3 axis*

For this class of motions,

$$\phi_0 = c^{-2}(\cosh\eta-\mu)^{\frac{1}{2}} \sum_{n=0}^{\infty} {}^{(t)}H_n^0 P_n^0 \exp[-(n+\tfrac{1}{2})\eta], \tag{4.13a}$$

$$\phi_1 = c^{-1} \cos\phi(\cosh\eta-\mu)^{\frac{1}{2}} \sum_{n=1}^{\infty} {}^{(t)}J_n^0 P_n^1 \exp[-(n+\tfrac{1}{2})\eta], \tag{4.13b}$$

$$\phi_2 = c^{-1} \sin\phi(\cosh\eta-\mu)^{\frac{1}{2}} \sum_{n=1}^{\infty} {}^{(t)}J_n^0 P_n^1 \exp[-(n+\tfrac{1}{2})\eta]. \tag{4.13c}$$

The resulting numerical calculations for this case confirm that with the exception of the $-{}_1F_3/\beta\alpha\,{}_1U_3 \equiv C$ resistance coefficient in (3.54), all of the remaining five U_3 coefficients of the first-order α_1 resistance matrix of (3.54) vanish identically. Values of C *vs.* κ resulting from these numerics are tabulated in table 2.

4.4. *Rotation about the x_1 axis*

In this case $p_j^{(r)}$ and $u_{kj}^{(r)}$ $(k,j = 1,2,3)$ are as given in (4.5)–(4.7), except that now the superscript (t) is replaced by (r), whilst the coefficients ${}^{(r)}A_n^m, {}^{(r)}B_n^m, \ldots, {}^{(r)}G_n^m$ are determined differently, through (3.6)–(3.10) and (3.16)–(3.18). Moreover, ϕ_0, ϕ_1 and ϕ_2 have the forms given in (4.8); however, the coefficients H_n^1, J_n^1 and K_n^1 now carry the superscript (r) rather than (t). Calculations of the first-order curvature effects upon the force and torque yielded the non-zero coefficients $-{}_1F_2/\beta\alpha\,{}_1\Omega_1 = -4G/3$, $-{}_1T_1/\beta\alpha\,{}_1\Omega_1 \equiv D$ of (3.54). These are tabulated in table 2 as a function of κ. As a consequence of the reciprocal theorem, the coefficient G is, of course, the same as that already derived in §4.2.

4.5. *Rotation about the x_2 axis*

Upon performing the requisite algebraic manipulations for this case – calculations that are by now familiar – and subsequently evaluating the integrals in (3.36) and

(3.37), we deduce the values of the non-zero first-order coefficients $-{}_1F_1/\beta\alpha\,{}_1\Omega_2 = 4H/3$ and $-{}_1T_2/\beta\alpha\,{}_1\Omega_2 = E$ appearing in (3.54). These are tabulated in table 2 *vs.* κ. The values of H obtained in this way accord with those derived in §4.1, such equality of coefficients being a consequence of the reciprocal theorem.

4.6. *Rotation about the x_3 axis*

In this case, ϕ_0, ϕ_1 and ϕ_2 retain the forms given in (4.13), except that now the superscripts (t) affixed to H_n^1 and J_n^1 are replaced by (r). $\overset{(r)}{H}{}_n^1$ and $\overset{(r)}{J}{}_n^1$ were then determined from an appropriate solution of (3.6)–(3.10) and (3.16)–(3.18). Evaluation of the integrals in (3.36) and (3.37) yielded only one non-zero Ω_3 coefficient, namely $-{}_1T_3/\beta\alpha\,{}_1\Omega_3 \equiv F$ in (3.54). Calculated values of this coefficient *vs.* κ are tabulated in table 2.

5. Sphere moving nearby to a spherical wall

As our first example of the application of the results of §§3 and 4 to specific wall geometries, consider a sphere S (physical radius = a) executing arbitrarily directed translational and rotational motions proximate to a larger sphere W (physical radius = R_o) for the case where $\beta = a/R_o \ll 1$ and $d/R_o \ll 1$. Interest centres on calculating the force and torque on the moving sphere for both the interior and exterior particle position cases, respectively depicted in figures 2(*a*) and 2(*b*). Discussion of these two examples is motivated by the availability of *exact* bipolar coordinate solutions of (the quasi-static) Stokes equations for both the internal and external sphere configurations, for all physically possible β and κ values. These allow a quantitative assessment of the accuracy of our asymptotic results, albeit only in the case where the boundary W is spherical.

In terms of the stretched Cartesian coordinate system introduced following (2.12), whose origin Q lies at the point of intersection of the line-of-centres of the two spherical surfaces with the spherical wall W, the non-dimensional equation of the latter boundary is

$$x_3 = \pm[\beta^{-1} - (\beta^{-2} - x_1^2 - x_2^2)^{\frac{1}{2}}] \quad \text{on } W. \tag{5.1}$$

Here and subsequently, the upper and lower signs refer to the respective cases where the moving sphere lies inside (figure 2*a*) or outside (figure 2*b*) of the stationary spherical surface W. For these two configurations we find from (5.1) and (3.43) that†

$$\alpha_1 = \alpha_2 = \pm 1. \tag{5.2}$$

Accordingly, (3.54) adopts the form

$$-\begin{pmatrix} F_1 \\ F_2 \\ F_3 \\ T_1 \\ T_2 \\ T_3 \end{pmatrix} = \left[\begin{array}{ccc|ccc} K_\perp^t & \cdot & \cdot & \cdot & -\frac{4}{3}K^c & \cdot \\ \cdot & K_\perp^t & \cdot & \frac{4}{3}K^c & \cdot & \cdot \\ \cdot & \cdot & K_\parallel^t & \cdot & \cdot & \cdot \\ \hline \cdot & K^c & \cdot & K_\perp^r & \cdot & \cdot \\ -K^c & \cdot & \cdot & \cdot & K_\perp^r & \cdot \\ \cdot & \cdot & \cdot & \cdot & \cdot & K_\parallel^r \end{array}\right] \begin{pmatrix} U_1 \\ U_2 \\ U_3 \\ \Omega_1 \\ \Omega_2 \\ \Omega_3 \end{pmatrix}, \tag{5.3}$$

† Equivalently, binomial expansion of (5.1) for $\beta \ll 1$ about the contact point Q, corresponding to $x_1 = x_2 = x_3 = 0$, yields

$$x_3 = \pm\tfrac{1}{2}\beta(x_1^2 + x_2^2) + O(\beta^3) \quad \text{on } W.$$

Direct comparison of this with (3.46) immediately furnishes the values of α_1 and α_2 set forth in (5.2).

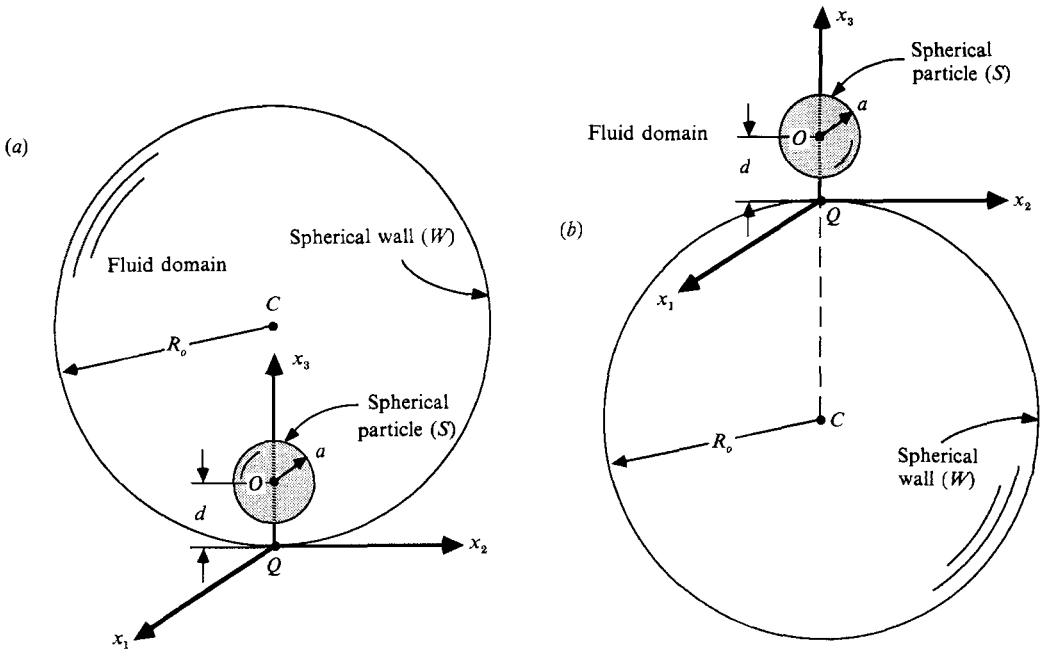

FIGURE 2. (*a*) Spherical particle S inside of a large sphere W. (*b*) Spherical particle S outside of a large sphere W.

wherein

$$K_{\perp}^{t} = a \pm (A+B)\beta + O(\beta^2), \tag{5.4a}$$

$$K_{\parallel}^{t} = b \pm 2C\beta + O(\beta^2), \tag{5.4b}$$

$$K_{\perp}^{r} = c \pm (D+E)\beta + O(\beta^2), \tag{5.4c}$$

$$K_{\parallel}^{r} = d \pm 2F\beta + O(\beta^2), \tag{5.4d}$$

$$K^{c} = e \mp (G+H)\beta + O(\beta^2). \tag{5.4e}$$

Equations (5.4), together with tables 1 and 2, furnish the five resistance coefficients, appearing in (5.3) in the form $K \equiv K(\kappa, \beta)$. These asymptotic results, valid only for $\beta \ll 1$ and $\kappa^{-1}\beta \ll 1$, may be compared with the exact bipolar-coordinate, two-sphere results available for the entire parametric range $0 < \beta < 1$ (and for all physically possible κ values) as discussed below.

5.1. *Translation and rotation perpendicular to the line of centres*

For this asymmetrical case, O'Neill & Majumdar (1970*a*) tabulate exact bipolar-coordinate-derived values of the three 'indirect' coefficients $K_{\perp}^{t}$, $K_{\perp}^{r}$ and K^{c} for all possible β and κ values. Included are both internal (figure 2*a*) and external (figure 2*b*) configurations. Their exact values† are compared in table 3 with our asymptotic results, derived from (5.4) together with tables 1 and 2.

† In the notation of O'Neill & Majumdar (1970*a*) these correspond to

$$f_{21} \equiv K_{\perp}^{t}, \quad g_{11} \equiv K_{\perp}^{r}, \quad g_{21} = 3f_{11}/4 \equiv -K^{c},$$

which depend functionally upon the parameters

$$\epsilon \equiv \Delta^{-1}, \quad \lambda = \pm\beta, \quad k = \beta^{-1},$$

with upper and lower signs respectively designating the internal and external cases.

		External				Internal	
		$\beta = 0.2$		$\beta = 0.25$		$\beta = 0.25$	
κ^{-1}		Eq. (5.4)	Exact	Eq. (5.4)	Exact	Eq. (5.4)	Exact
1.5	$K_\perp^t$	1.4072	1.3657	—	—	—	—
	$K_\perp^r$	1.1097	1.0877	—	—	—	—
	K^c	0.0561	0.0506	—	—	—	—
1.4	$K_\perp^t$	—	—	1.3982	1.3867	1.9528	2.7870
	$K_\perp^r$	—	—	1.1368	1.1097	1.1493	1.2075
	K^c	—	—	0.0802	0.0666	−0.0349	−0.1306
1.05	$K_\perp^t$	1.9652	2.0543	—	—	—	—
	$K_\perp^r$	1.6164	1.5566	—	—	—	—
	K^c	0.2587	0.2319	—	—	—	—
1.005	$K_\perp^t$	2.5522	2.8464	—	—	—	—
	$K_\perp^r$	2.2860	2.2593	—	—	—	—
	K^c	0.5501	0.4962	—	—	—	—

TABLE 3. Resistance coefficients for a small spherical particle translating and/or rotating about an axis lying parallel to the tangent plane of a nearby spherical wall, equivalent to motion about an axis lying perpendicular to the line of centres of the two spheres.

For the external case the agreement is generally quite good, especially when it is considered that the β values for which the comparison is made can hardly be said to satisfy the assumed inequalities, $\beta \ll 1$ and $\kappa^{-1}\beta \ll 1$. Agreement between the asymptotic and exact results is not nearly so satisfactory for the internal case. This disparity can be attributed in part to the fact that the β value (for which comparison was possible) was not small, and in part to the fact that the vanishing velocity boundary condition (2.22) imposed at infinity upon the first-order field (2.19)–(2.22) introduces a significant error into the physically bounded internal case, except of course when $\beta \ll 1$ strictly.

5.2. *Translation and rotation parallel to the line of centres*

Exact bipolar results for the remaining sphere/sphere coefficients $K_\parallel^t$ and $K_\parallel^r$ were obtained by extending the axisymmetric analysis of Stimson & Jeffery (1926).† These exact results are compared in table 4 with the asymptotic $\beta \ll 1$ results derived jointly from (5.4) and tables 1 and 2. As expected, the agreement is quite good at the smaller β value ($\beta = 0.05$) and less so at the larger one ($\beta = 0.20$). Moreover, for the same β value, agreement is substantially better for the external case than for the

† After completing these bipolar calculations, we became aware of the comparable analyses of Cooley & O'Neill (1969*a*, *b*) for $K_\parallel^t$ and Majumdar (1965, 1969) for $K_\parallel^r$. For those few common choices of parametric values of β and κ permitting comparison with our $K_\parallel^t$ values, quite good agreement was observed. For example, in the internal case, and with $\beta = 0.2$, the values given by Cooley & O'Neill (1969*b*) (corresponding to one-half of the values tabulated in *their* table 3), were, respectively, 5.0627 ($\kappa^{-1} = 1.4$), 16.7018 ($\kappa^{-1} = 1.1$) and 32.2660 ($\kappa^{-1} = 1.05$) *vs.* our 'exact' values, tabulated in table 4. Likewise, in the external case, and for $\beta = 0.2$ and $\kappa^{-1} = 1.05$, Cooley & O'Neill (1969*b*) give $K_\parallel^t = 15.5903$ *vs.* our exact table 4 value. In general, agreement obtains to within at least several parts in ten thousand.

Except for the special case of tangent spheres (i.e. $\kappa = 1$) treated by Majumdar (1969), the exact bipolar-coordinate results for $K_\parallel^r$ (Majumdar 1965) were not accessible to us. However, comparison of Majumdar's (1969) tangent-sphere 'lubrication' results with those of our analysis are made at the end of this section.

		External				Internal			
		$\beta = 0.05$		$\beta = 0.20$		$\beta = 0.05$		$\beta = 0.20$	
κ^{-1}		Eq. (5.4)	Exact	Eq. (5.4)	Exact	Eq. (5.4)	Exact	Eq. (5.4)	Exact
3.0	$K_{\parallel}^{t}$	1.5162	1.5113	—	—	1.6222	1.6410	—	—
	$K_{\parallel}^{r}$	1.0039	1.0037	—	—	1.0054	1.0060	—	—
2.0	$K_{\parallel}^{t}$	2.0329	2.0292	1.7553	1.8140	2.2181	2.2399	2.4957	2.7534
	$K_{\parallel}^{r}$	1.0140	1.0137	1.0085	1.0092	1.0178	1.0186	1.0233	1.0316
1.6	$K_{\parallel}^{t}$	2.7026	2.6986	2.2636	2.3549	2.9952	3.0243	3.4342	3.7760
	$K_{\parallel}^{r}$	1.0287	1.0282	1.0193	1.0201	1.0349	1.0361	1.0443	1.0549
1.4	$K_{\parallel}^{t}$	3.5192	3.5156	2.8699	3.0075	3.9520	3.9912	4.6013	5.0631
	$K_{\parallel}^{r}$	1.0440	1.0439	1.0293	1.0324	1.0538	1.0548	1.0685	1.0792
1.2	$K_{\parallel}^{t}$	5.9076	5.9050	4.6077	4.8905	6.7742	6.8452	8.0741	8.9368
	$K_{\parallel}^{r}$	1.0748	1.0756	1.0495	1.0577	1.0916	1.0919	1.1169	1.1271
1.1	$K_{\parallel}^{t}$	10.5830	10.5803	7.9542	8.5296	12.3354	12.4830	14.9642	16.7034
	$K_{\parallel}^{r}$	1.1073	1.1069	1.0778	1.0828	1.1269	1.1286	1.1564	1.1743
1.05	$K_{\parallel}^{t}$	19.9086	19.8107	14.8771	15.6647	23.2630	23.6701	28.2945	32.2892
	$K_{\parallel}^{r}$	1.1338	1.1328	1.0998	1.1035	1.1564	1.1591	1.1904	1.2139
1.025	$K_{\parallel}^{t}$	38.3277	38.1186	28.1441	29.762	45.1167	46.0063	55.3003	63.5439
	$K_{\parallel}^{r}$	1.1528	1.1519	1.1140	1.1187	1.1788	1.1816	1.2176	1.2435

TABLE 4. Resistance coefficients for a small spherical particle translating and/or rotating about an axis lying perpendicular to the tangent plane of a nearby spherical wall, equivalent to motion parallel to the line of centres joining the two spheres.

internal one, as was also observed to occur for the asymmetrical sphere motions of table 3. The rationalization advanced in that context to explain this phenomenon remains equally true in the present symmetrical case.

5.3. '*Lubrication-theory*' *asymptotes* ($\kappa \to 1$)

Asymptotic results for this $\Delta \gg 1$ case, involving two unequal spheres in both internal and external configurations, are given: (i) by O'Neill & Majumdar (1970*b*) for asymmetric motions as

$$K_{\perp}^{t} = \frac{4(2 \mp \beta + 2\beta^2)}{15(1 \mp \beta)^3} \ln \Delta + O(1), \tag{5.5a}$$

$$K_{\perp}^{r} = \frac{2}{5(1 \mp \beta)} \ln \Delta + O(1), \tag{5.5b}$$

$$K^{c} = \frac{(1 \mp 4\beta)}{10(1 \mp \beta)^2} \ln \Delta + O(1); \tag{5.5c}$$

(ii) by Cooley & O'Neill (1969*b*) for the symmetrical translational case as

$$K_{\parallel}^{t} = \frac{\Delta}{(1 \mp \beta)^2} + \frac{1 \mp 7\beta + \beta^2}{5(1 \mp \beta)^2} \ln \Delta + O(1); \tag{5.5d}$$

and (iii) by Majumdar (1969) for the symmetrical rotation case as

$$K_{\parallel}^{r} = \sum_{n=0}^{\infty} [(n+1) \mp n\beta]^{-3} + O(\Delta^{-1}). \tag{5.5e}$$

Note that the leading term of the latter represents the exact tangent-sphere (i.e. $\Delta^{-1} = 0$) result, which is non-singular. As usual, the upper and lower signs in each of (5.5) apply respectively to the internal and external modes.

Each of these five asymptotic results is valid for *all* β. Upon expansion for $\beta \ll 1$, these results are readily shown to conform exactly with our (5.4) small-gap counterparts upon utilizing the $\Delta^{-1} \to 0$ asymptotes displayed in the last rows of tables 1 and 2, the latter values having been derived independently (see the Appendix) from the general lubrication-theory analysis of Cox (1974) for arbitrary, generally non-spherical surfaces in close proximity.

The only comparison requiring further elaboration stems from the expansion of (5.5*e*) for small β. Binomial expansion of the latter yields

$$K_{\parallel}^{\mathrm{r}} = \zeta(3) \pm 3[\zeta(3) - \zeta(4)]\beta + O(\beta^2), \tag{5.6}$$

wherein

$$\zeta(\nu) = \sum_{n=0}^{\infty} (n+1)^{-\nu}$$

is the Riemann zeta function (Abramowitz & Stegun 1964). Numerically,

$$K_{\parallel}^{\mathrm{r}} = 1.2021 \pm 0.3592\beta + O(\beta^2), \tag{5.7}$$

in conformity with (5.4*d*).

Observe that the algebraic signs of the β coefficients appearing in (5.5) explicitly confirm our previous speculation that, for the asymptotic $\beta \ll 1$ case, the errors incurred for the internal configuration case will always exceed those for the external configuration case at the same value of β. Additionally, (5.5*c*) shows that the coupling coefficient K^{c} for the internal mode undergoes a change in algebraic sign at $\beta \approx 0.25$, at least in the lubrication-theory limit (but see table 3 for more general confirmation of this fact). This sensitivity in the neighbourhood of $\beta \approx 0.25$ also suggests why the percentage error in K^{c} for this β value (see table 3) is so much larger for the internal mode than the external one. The importance of this change of algebraic sign in the internal-mode coupling coefficient K^{c} for the spherical-outer-boundary case relates closely to the slip-velocity calculation of (6.12) for the circular-cylindrical-outer-boundary case, discussed in §6.

6. Sphere moving near a circular cylindrical wall

In terms of applications, the most commonly encountered boundary shape is that of an infinitely extended circular cylinder (containing the spherical particle in its interior). This section applies the generic results of §§3 and 4 to this specific case (more generally to *both* internal and external sphere motions), and subsequently uses the explicit results obtained to resolve the 'paradox' described in the Introduction – which problem motivated our original efforts.

In the notation of the stretched Cartesian coordinate system introduced following (2.12), the equation defining the cylinder wall W (with x_2 as the longitudinal cylinder axis) is

$$x_3 = \pm[\beta^{-1} - (\beta^{-2} - x_1^2)^{\frac{1}{2}}] \quad \text{on } W. \tag{6.1}$$

Here, and subsequently, the upper or lower signs apply according as the sphere is located inside (figure 3*a*) or outside (figure 3*b*) of the cylinder. From (6.1) and (3.43) (see also the footnote to (5.2)) it follows that

$$\alpha_1 = \pm 1, \quad \alpha_2 = 0. \tag{6.2a,b}$$

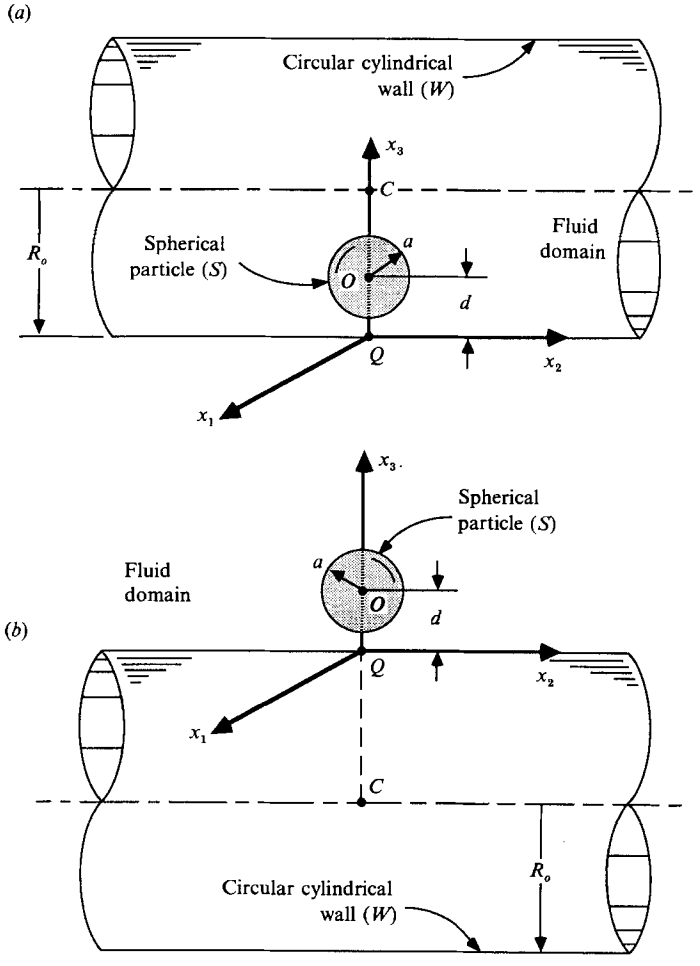

FIGURE 3. (*a*) Spherical particle S inside of a large circular cylinder W. (*b*) Spherical particle S outside of a large circular cylinder W.

Accordingly, (3.54) may be written in the form

$$-\begin{bmatrix} F_1 \\ F_2 \\ F_3 \\ T_1 \\ T_2 \\ T_3 \end{bmatrix} = \left[\begin{array}{ccc|ccc} K_{11}^{t} & \cdot & \cdot & \cdot & -\tfrac{4}{3}K_{21}^{c} & \cdot \\ \cdot & K_{22}^{t} & \cdot & \tfrac{4}{3}K_{12}^{c} & \cdot & \cdot \\ \cdot & \cdot & K_{33}^{t} & \cdot & \cdot & \cdot \\ \hline \cdot & K_{12}^{c} & \cdot & K_{11}^{r} & \cdot & \cdot \\ -K_{21}^{c} & \cdot & \cdot & \cdot & K_{22}^{r} & \cdot \\ \cdot & \cdot & \cdot & \cdot & \cdot & K_{33}^{r} \end{array}\right] \begin{bmatrix} U_1 \\ U_2 \\ U_3 \\ \Omega_1 \\ \Omega_2 \\ \Omega_3 \end{bmatrix}, \tag{6.3}$$

in which

$$K_{11}^{t} = a \pm A\beta + O(\beta^2), \quad K_{22}^{t} = a \pm B\beta + O(\beta^2), \quad K_{33}^{t} = b \pm C\beta + O(\beta^2), \tag{6.4a,b,c}$$

$$K_{11}^{r} = c \pm D\beta + O(\beta^2), \quad K_{22}^{r} = c \pm E\beta + O(\beta^2), \quad K_{33}^{r} = d \pm F\beta + O(\beta^2), \tag{6.4d,e,f}$$

$$K_{12}^{c} = e \mp G\beta + O(\beta^2), \quad K_{21}^{c} = e \mp H\beta + O(\beta^2). \tag{6.4g,h}$$

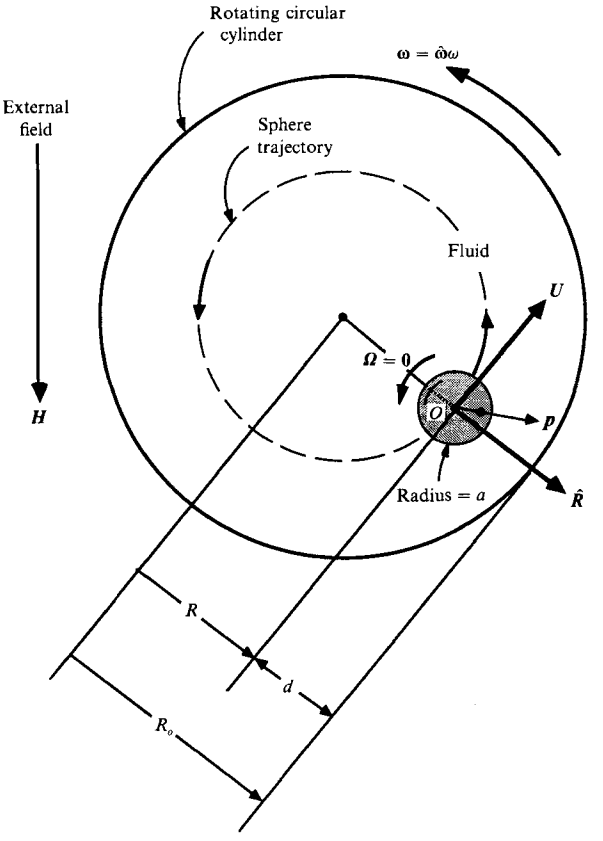

FIGURE 4. Force-free dipolar sphere (radius = a) containing an embedded dipole $\boldsymbol{p}$ and suspended within a large fluid-filled circular cylinder of radius R_o that is rotating with angular velocity $\boldsymbol{\omega}$ about its longitudinal axis which lies perpendicular to an external field $\boldsymbol{H}$.

The preceding expressions furnish each of the eight non-zero resistance coefficients $K_{ij}^{(\cdot)}$ as explicit functions of κ and β. Since all of the coefficients $a(\kappa), b(\kappa), \ldots, G(\kappa)$, $H(\kappa)$ tabulated in tables 1 and 2 are non-negative for all κ, (6.4) shows that for the internal case all of the six 'direct' translational and rotational coefficients increase with increasing β, whereas the two 'indirect' coupling coefficients decrease with increasing β. The converse holds for the external case, where the sphere lies outside of the cylinder.

6.1. *Dipolar sphere in a rotating circular cylinder*

As in figure 4 we consider a fluid-filled circular cylinder of radius R_o rotating symmetrically with angular velocity $\boldsymbol{\omega}$ about its longitudinal axis. Situated with its centre O at a distance $R = R_o - d$ from the cylinder axis is an otherwise neutrally buoyant spherical particle of radius a containing an embedded vector dipole $\boldsymbol{p}$ permanently locked into the sphere. When a (space-fixed) uniform external field $\boldsymbol{H}$ exists, an external couple

$$\boldsymbol{T}^{(e)} = \boldsymbol{p} \times \boldsymbol{H} \tag{6.5}$$

acts on the sphere, tending to align the dipole parallel to the field. In its absence the sphere would simply participate in the otherwise rigid-body rotation occurring within the cylinder interior, with its centre O translating with velocity $\boldsymbol{\omega} \times \boldsymbol{R}$ whilst

the sphere rotates about an axis through its centre with angular velocity $\boldsymbol{\omega}$; here, $\boldsymbol{R} = \hat{\boldsymbol{R}}R$ is the position vector of the sphere centre relative to the cylinder axis, with $\hat{\boldsymbol{R}}$ a unit vector.

Owing, however, to the action of the external couple, such unconstrained motion of the sphere is no longer possible (except trivially), whence the translational velocity $\boldsymbol{U}$ of the sphere centre and the angular velocity $\boldsymbol{\Omega}$ of the sphere will no longer conform to their rigid-body values. In order to calculate these constrained velocities we write

$$\boldsymbol{F} = -\mu[\boldsymbol{K}^{\mathrm{t}} \cdot (\boldsymbol{U} - \boldsymbol{\omega} \times \boldsymbol{R}) + \boldsymbol{K}^{\mathrm{c}\P} \cdot (\boldsymbol{\Omega} - \boldsymbol{\omega})] \tag{6.6}$$

and

$$\boldsymbol{T} = -\mu[\boldsymbol{K}^{\mathrm{c}} \cdot (\boldsymbol{U} - \boldsymbol{\omega} \times \boldsymbol{R}) + \boldsymbol{K}^{\mathrm{r}} \cdot (\boldsymbol{\Omega} - \boldsymbol{\omega})] \tag{6.7}$$

for the Stokes force and torque (about the sphere centre). In contrast to prior notation, all quantities appearing in (6.6) and (6.7) possess their physical (dimensional) values. In particular, the dimensional hydrodynamic resistance dyadics appearing in (6.6) and (6.7) are related to the non-dimensional resistance components appearing in (6.4) by the expressions

$$\boldsymbol{K}^{\mathrm{t}} = 6\pi a(\boldsymbol{i}_1 \boldsymbol{i}_1 K^{\mathrm{t}}_{11} + \boldsymbol{i}_2 \boldsymbol{i}_2 K^{\mathrm{t}}_{22} + \boldsymbol{i}_3 \boldsymbol{i}_3 K^{\mathrm{t}}_{33}), \tag{6.8a}$$

$$\boldsymbol{K}^{\mathrm{c}} = 8\pi a^2(\boldsymbol{i}_1 \boldsymbol{i}_2 K^{\mathrm{c}}_{12} - \boldsymbol{i}_2 \boldsymbol{i}_1 K^{\mathrm{c}}_{21}), \tag{6.8b}$$

$$\boldsymbol{K}^{\mathrm{r}} = 8\pi a^3(\boldsymbol{i}_1 \boldsymbol{i}_1 K^{\mathrm{r}}_{11} + \boldsymbol{i}_2 \boldsymbol{i}_2 K^{\mathrm{r}}_{22} + \boldsymbol{i}_3 \boldsymbol{i}_3 K^{\mathrm{r}}_{33}). \tag{6.8c}$$

Consistent with the definitions of the unit vectors $(\boldsymbol{i}_1, \boldsymbol{i}_2, \boldsymbol{i}_3)$ implicit in figure 3(*a*), we have that (see figure 4)

$$\boldsymbol{i}_1 = \hat{\boldsymbol{\omega}} \times \hat{\boldsymbol{R}}, \quad \boldsymbol{i}_2 = -\hat{\boldsymbol{\omega}}, \quad \boldsymbol{i}_3 = -\hat{\boldsymbol{R}}, \tag{6.9a,b,c}$$

with $\hat{\boldsymbol{\omega}} \overset{\text{def}}{=} \boldsymbol{\omega}/\omega$ a unit vector, and $\omega = |\boldsymbol{\omega}|$.

Owing to the absence of any net external force $\boldsymbol{F}^{(\mathrm{e})}$ acting on the sphere, together with the fact that $\boldsymbol{F} + \boldsymbol{F}^{(\mathrm{e})} = \boldsymbol{0}$, we have that $\boldsymbol{F} = \boldsymbol{0}$ in (6.6).† Following the original example (Brenner 1984) leading up to the present calculations, further attention will be confined to circumstances for which: (i) the external field $\boldsymbol{H}$ is perpendicular to the cylinder axis ($\hat{\boldsymbol{H}} \cdot \hat{\boldsymbol{\omega}} = 0$); (ii) the sphere does not rotate about its own axis ($\boldsymbol{\Omega} = \boldsymbol{0}$), corresponding to the case where the non-dimensional parameter $pH/8\pi\mu a^3\omega$ exceeds a threshold value (of unity in the case where wall effects are negligible). This occurs either for large fields $H = |\boldsymbol{H}|$ (not to be confused with the wall-effect coefficient H) or slow rotation speeds ω. Physically, the dipole vector $\boldsymbol{p}$ lies in the plane of figure 4, somewhere between the 6 o'clock position it possesses when $\omega = 0$ and the 3 o'clock position it attains at the threshold value. (Below this threshold value the non-rotating case $\boldsymbol{\Omega} = \boldsymbol{0}$ is no longer possible, and the sphere undergoes an unsteady rotation (Brenner 1984).)

Upon setting $\boldsymbol{F} = \boldsymbol{0}$ and $\boldsymbol{\Omega} = \boldsymbol{0}$ in (6.6) and solving for $\boldsymbol{U}$, we obtain

$$\boldsymbol{U} - \boldsymbol{\omega} \times \boldsymbol{R} = (\boldsymbol{K}^{\mathrm{t}})^{-1} \cdot \boldsymbol{K}^{\mathrm{c}\P} \cdot \boldsymbol{\omega}. \tag{6.10}$$

Upon use of (6.8) and (6.9) this yields

$$\boldsymbol{U} = \boldsymbol{\omega} \times \boldsymbol{R}(1 + \hat{U}_{\mathrm{s}}), \tag{6.11}$$

with

$$\hat{U}_{\mathrm{s}} = \frac{4}{3} \frac{a}{R_o - d} \frac{K^{\mathrm{c}}_{21}}{K^{\mathrm{t}}_{11}} \tag{6.12}$$

† Additionally, $\boldsymbol{T} = -\boldsymbol{T}^{(\mathrm{e})} \neq \boldsymbol{0}$, where $\boldsymbol{T}^{(\mathrm{e})}$ is given by (6.5). However, we shall not explicitly use (6.7).

the non-dimensional 'slip' velocity of the sphere (centre). Thus, the sphere centre traverses the same circular trajectory as it would in the absence of the dipole (or field), except that now, owing to the existence of the latter in conjunction with wall effects, the sphere will translate faster or slower than the undisturbed rigid-body motion occurring in its proximity according as $\hat{U}_s$ is positive or negative. Accordingly, the algebraic sign of this slip velocity acquires heightened importance in terms of this departure from simple rigid-body rotation.

With use of (6.4) (for the internal case), the slip velocity (6.12) can be expressed in the form

$$\hat{U}_s(\kappa;\beta) \sim \frac{4}{3}\frac{\beta}{1-\kappa^{-1}\beta}\frac{e(\kappa)-H(\kappa)\beta}{a(\kappa)+A(\kappa)\beta}, \tag{6.13}$$

at least for $\beta \ll 1$. (Note that the inequality $1-\kappa^{-1}\beta > 0$ always holds for the internal case.) For any given β, (6.13) permits investigation of how the slip velocity varies with the radial position κ of the sphere. Of course, our entire calculation pertains only to the case where the sphere is relatively close to the cylinder wall, namely

$$d/R_o = \kappa^{-1}\beta \ll 1. \tag{6.14}$$

Observe from (6.13) that, as regards the algebraic sign of the slip velocity for the present internal case,

$$\operatorname{sgn} \hat{U}_s = \operatorname{sgn}[e(\kappa)-H(\kappa)\beta]. \tag{6.15}$$

Two limiting cases are of special interest to us in relation to our previous (Brenner 1984) incomplete discussion of the slip.

Case (*i*) Plane-wall approximation:

$$\beta \ll 1, \quad \kappa = O(1). \tag{6.16a,b}$$

This limit gives rise to the so-called flat-wall approximation. In this limit (which clearly satisfies the inequality (6.14) automatically), (6.13) reduces to

$$\hat{U}_s \sim \tfrac{4}{3}\beta\frac{e(\kappa)}{a(\kappa)} > 0. \tag{6.17}$$

The algebraic sign of this slip velocity is a consequence of the non-negative nature of e and a, displayed in table 1.

Case (*ii*) Hirschfeld *et al.* (1984)/Falade & Brenner (1985) 'reflection' approximation:

$$\beta \ll 1, \quad \kappa \ll 1. \tag{6.18a,b}$$

From the $\kappa \to 0$ asymptotes tabulated in the first rows of tables 1 and 2, (6.13) here reduces to

$$\hat{U}_s \sim \tfrac{1}{96}\beta\kappa(16\kappa^3 - 9\beta). \tag{6.19}$$

For example, the choice

$$\kappa = O(\beta^{1-\epsilon}) = L\beta^{1-\epsilon}, \tag{6.20}$$

say, with L an $O(1)$ constant, and ϵ chosen to lie in the range

$$\tfrac{2}{3} > \epsilon > 0, \tag{6.21}$$

will satisfy inequalities (6.18*b*) and (6.14), while simultaneously furnishing the strong inequality $9\beta \gg 16\kappa^3$ for the specified parametric range. Hence, in such circumstances,

$$\hat{U}_s = -\tfrac{3}{32}L\beta^{3-\epsilon} < 0, \tag{6.22}$$

whence the slip velocity is negative. When the inequality (6.21) holds, the β-dependence of the slip velocity varies between $O(\beta^{\frac{7}{3}})$ and $O(\beta^3)$, whereas in (6.17) the dependence is of $O(\beta)$. Insofar as magnitude is concerned, the latter constitutes a much larger wall effect than does the former.

It follows from these considerations that (for a fixed β) as the sphere moves from the inner wall region $\kappa = O(1)$ to the outer wall region $\kappa \ll 1$, the sphere changes from leading to lagging the fluid in which it is suspended. At the same time, the *magnitude* of this slip velocity diminishes. This slowing down of the suspended particles with increasing distance from the wall does not occur abruptly, but rather gradually. Indeed, from (6.13) we see that at the radial distance κ given by $\epsilon(\kappa)/H(\kappa) = \beta$ no slip velocity occurs at all. For the $\kappa \ll 1$ case, (6.19) shows that this occurs when the sphere centre is situated at the dimensionless position

$$\kappa = (9\beta/16)^{\frac{1}{3}}. \tag{6.23}$$

As regards the basic physics of the problem, we believe that the change in algebraic sign of the slip velocity with increasing distance of the sphere centre from the wall arises from the fact that it then begins to feel the presence of the opposite side of the rotating cylinder due to the long-range wall effects characteristic of Stokes flows.

These general facts are important in connection with the possible existence and algebraic sign of the slip velocity occurring at the wall of an otherwise stationary ferrofluid suspension in the presence of a rotating magnetic field (Rosensweig 1982; Brenner 1984). Further work will be necessary to transform our single-particle analysis into a form suitable for dealing with suspensions, or attempting to incorporate Brownian motion effects (as well as $\boldsymbol{\Omega} \neq \mathbf{0}$ effects) into a complete analysis of the phenomenon.

This research was jointly supported by the US National Science Foundation and the US Army Chemical Research and Development Center.

Appendix. Asymptotic resistance coefficients

In this Appendix we outline the sources for the respective $\kappa \to 0$ and $\kappa \to 1$ hydrodynamic resistance asymptotes tabulated in the first and last rows of tables 1 and 2 as representing the respective plane wall $[O(\beta^0)]$ and first-order $[O(\beta)]$ wall-curvature resistance coefficients for the sphere in proximity to a bounding wall.

A.1. '*Reflection*' *results:* $\kappa \to 0$

A.1.1. $O(\beta^0)$. The asymptotic expressions appearing in the $\kappa^{-1} \to \infty$ row of table 1 derive from reflection-type analyses (Lorentz 1896) of the translational and rotational motions of a spherical particle moving far from a plane wall bounding a semi-infinite quiescent fluid. These results are summarized by Goldman *et al.* (1967*a*).

A.1.2. $O(\beta)$. These first-order coefficients, appearing in the $\kappa^{-1} \to \infty$ row of table 2, derive directly from the reflection analyses of Hirschfeld *et al.* (1984) and Falade & Brenner (1985).

A.2. '*Lubrication*' *results:* $\kappa \to 1$

A.2.1. $O(\beta^0)$. Asymptotic expressions for the κ-dependence of the coefficients a, c and e, given in the $\kappa^{-1} \to 1$ row of table 1, derive from the independent analyses of O'Neill & Stewartson (1967) and Goldman *et al.* (1967*a*) for the translational and

rotational motions of a sphere parallel to a nearby plane wall bounding a semi-infinite, otherwise quiescent fluid.

Comparable expressions for the remaining two coefficients, b and d, derive respectively from the solutions of Cox & Brenner (1967*b*) for the axisymmetric translation of a body of revolution normal to a plane wall in the small-gap limit, and from the symmetrical rotation about an axis normal to a plane wall of a sphere whose surface is tangent to the wall. Note that the latter d coefficient is non-singular in this limit.

A.2.2. $O(\beta)$. With the exception of the F coefficient appearing in the $\kappa^{-1} \to 1$ row of table 2, which is non-singular in the $\kappa = 1$ limit, the remaining singular $\Delta^{-1} \to 0$ coefficients were derived from the general 'lubrication-theory' analysis of Cox (1974) for the relative translational and rotational closely proximate motions of two smooth surfaces, each of arbitrary curvature, and separated by a narrow fluid-filled gap (whose minimum thickness is small compared with each of the four principal radii of curvature characterizing the two surfaces in the neighbourhood of the gap). Cox's (1974) analysis, which yields all the singular, lubrication-type terms, is not restricted to small β, but rather applies more generally† in the sense of (5.5) *vs.* (5.4). Nevertheless, we have used only the $\beta \ll 1$ aspects of his work (obtained by binomial expansion) in deriving the asymptotic results set forth in table 2. Simultaneously, the leading term [of $O(\beta^0)$] in this expansion furnishes independent confirmation of the comparable plane-wall asymptotic results set forth for each of the singular coefficients in the $\kappa^{-1} \to 1$ row of table 1.

In the course of obtaining these $O(\beta^0)$ and $O(\beta)$ singular coefficients, Cox's (1974) expressions for the intrinsic hydrodynamic resistance dyadics – originally given by him in terms of an origin situated at the contact point (point Q in figure 1) – were transformed by us into the comparable resistance dyadics for an origin situated at the centre O of the moving sphere. This transition was effected by using the origin-transformation formulas of Brenner (1964*a*) (see also Happel & Brenner 1965, pp. 173–175), which transformation formulas apply equally well to the present wall-effect case (owing to the zero-velocity boundary condition on W).

In deriving the asymptotic non-singular F term in table 2 for the tangent case, $\kappa = 1$ – which $O(1)$ term is *not* explicitly given by Cox's (1974) analysis – we employed the binomial expansion of Majumdar's (1967) exact equation (5.5*e*) for the case $\beta \ll 1$ (cf. (5.6) and (5.7)), arising from the symmetric rotation of two unequal spheres in contact. This permitted us to compare (5.7) directly with (5.4*d*) and so obtain the limiting value, $F = 0.17960$, given in table 2. (Of course this same comparison simultaneously confirmed the non-singular $d = 1.2021$ value given for the $O(\beta^0)$ term in the $\kappa^{-1} \to 1$ row of table 1.) The limiting F (and d) value(s) derived in this manner from the spherical-wall analysis apply, of course, to the more general case where the wall W possesses arbitrary curvatures α_1 and α_2 in (3.54); for the tabulated values given in tables 1 and 2 are independent of the explicit shape of W – in particular of whether or not W is spherical.

As a check of the accuracy of some of our numerical results, the entries in table 2 for A, B, D, E and H at $\kappa^{-1} = 1.025$ and 1.005 were used to estimate the multiplicands of the logarithmic terms appearing in the asymptotic expressions for these $O(\beta)$ coefficients as $\kappa^{-1} \to 1$. The approximate values of the multiplicands so obtained are compared in table 5 with the exact logarithmic coefficients given in the last row of table 2.

† For the special case where both of Cox's surfaces are spherical we have confirmed that the non-small β results of (5.5) are properly reproduced by Cox's equations.

	Multiplicand of log term	
Coefficient	Approximate value	Exact value
A	0.986	$74/75 \equiv 0.987$
B	0.338	$26/75 \equiv 0.347$
D	0.269	$13/50 \equiv 0.260$
E	0.134	$7/50 \equiv 0.140$
H	0.181	$19/100 \equiv 0.190$

TABLE 5. Comparison of numerically estimated logarithmic coefficients with analytical values of these coefficients for selected $\kappa^{-1} > 1$ terms in table 2.

It did not prove possible to carry out a similar exercise for G because its rate of approach to its asymptotic logarithmic value as $\kappa^{-1} \to 1$ is much slower than those of A, B, D, E and H.

The non-singular, higher-order terms appearing in the asymptotic $\Delta \to \infty$ expansions for the quantities A, B, D, E, G and H, given in the last row of table 2, were numerically estimated from the respective $\kappa^{-1} = 1.005$ tabulations for these quantities. For C, the estimated multiplicands of the respective $\Delta^{\frac{1}{2}}$ and $\ln \Delta$ terms were obtained from the tabulated C values at $\kappa^{-1} = 1.025$ and $\kappa^{-1} = 1.005$ in table 2. Finally, the estimated multiplicand of the Δ^{-1} coefficient in the expansion of the non-singular F function in table 2 was derived from the tabulated F value at $\kappa^{-1} = 1.005$.

REFERENCES

ABRAMOWITZ, M. & STEGUN, I. A. 1964 *Handbook of Mathematical Functions*, pp. 807, 811. US Govt. Printing Office, Washington, DC.

ADEROGBA, K. 1977 On eigen stresses in dissimilar media. *Phil. Mag. A* **35**, 281–292.

BRENNER, H. 1961 The slow motion of a sphere through a viscous fluid towards a plane surface. *Chem. Engng Sci.* **16**, 242–251.

BRENNER, H. 1964*a* The Stokes resistance of an arbitrary particle. II. An extension. *Chem. Engng Sci.* **19**, 599–629.

BRENNER, H. 1964*b* The Stokes resistance of an arbitrary particle. IV. Arbitrary fields of flow. *Chem. Engng Sci.* **19**, 703–727.

BRENNER, H. 1966 Hydrodynamic resistance of particles at small Reynolds numbers. *Adv. Chem. Engng* **6**, 287–438.

BRENNER, H. 1972 Dynamics of neutrally buoyant particles in low Reynolds number flows. *Prog. Heat Mass Transfer* **6**, 509–574.

BRENNER, H. 1984 Antisymmetric stresses induced by the rigid-body rotation of dipolar suspensions: Vortex flows. *Intl J. Engng Sci.* **22**, 645–682.

BUNGAY, P. M. & BRENNER, H. 1973 The motion of a closely-fitting sphere in a fluid-filled tube. *Intl J. Multiphase Flow* **1**, 25–56.

COOLEY, M. D. A. 1971 The slow rotation in a viscous fluid of a sphere close to another fixed sphere about a diameter perpendicular to the line of centers. *Q. J. Mech. Appl. Maths* **24**, 237–250.

COOLEY, M. D. A. & O'NEILL, M. E. 1968 On the slow rotation of a sphere about a diameter parallel to a nearby plane wall. *J. Inst. Maths Applics* **4**, 163–173.

COOLEY, M. D. A. & O'NEILL, M. E. 1969*a* On the slow motion of two spheres in contact along their line of centres through a viscous fluid. *Proc. Camb. Phil. Soc.* **66**, 407–415.

COOLEY, M. D. A. & O'NEILL, M. E. 1969*b* On the slow motion generated in a viscous fluid by the approach of a sphere to a plane wall or stationary sphere. *Mathematika* **16**, 37–49.

Cox, R. G. 1974 The motion of suspended particles almost in contact. *Intl J. Multiphase Flow* **1**, 343–371.

Cox, R. G. & Brenner, H. 1967*a* Effect of finite boundaries on the Stokes resistance of an arbitrary particle. III. Translation and rotation. *J. Fluid Mech.* **28**, 391–411.

Cox, R. G. & Brenner, H. 1967*b* The slow motion of a sphere through a viscous fluid towards a plane surface. II. Small gap widths, including inertial effects. *Chem. Engng Sci.* **22**, 1753–1777.

Davis, M. H. 1969 The slow translation and rotation of two unequal spheres in a viscous fluid. *Chem. Engng Sci.* **24**, 1769–1776.

Dean, W. R. & O'Neill, M. E. 1963 A slow motion of viscous liquid caused by the rotation of a sphere. *Mathematika* **10**, 13–24.

Falade, A. & Brenner, H. 1985 Stokes wall effects for particles moving near cylindrical boundaries. *J. Fluid Mech.* **154**, 145–162.

Gibbs, J. W. & Wilson, E. B. 1960 *Vector Analysis*, pp. 411–419. Dover (reprint).

Gluckman, M. J., Pfeffer, R. & Weinbaum, S. 1971 New technique for treating multiparticle slow viscous axisymmetric flow past spheres and spheroids. *J. Fluid Mech.* **50**, 705–740.

Goldman, A. J., Cox, R. G. & Brenner, H. 1967*a* Slow viscous motion of a sphere parallel to a plane wall. I. Motion through a quiescent fluid. *Chem. Engng Sci.* **22**, 637–651.

Goldman, A. J., Cox, R. G. & Brenner, H. 1967*b* Slow viscous motion of a sphere parallel to a plane wall. II. Couette flow. *Chem. Engng Sci.* **22**, 653–660.

Goldsmith, H. L. & Skalak, R. 1975 Hemodynamics. *Ann. Rev. Fluid Mech.* **7**, 213–247.

Gradshteyn, I. S. & Ryzhik, I. M. 1980 *Tables of Integrals, Series and Products*. Academic.

Happel, J. & Brenner, H. 1965 *Low Reynolds Hydrodynamics*. Prentice-Hall (reprinted 1973, Noordhoff, Leyden, The Netherlands).

Hasimoto, H. & Sano, D. 1980 Stokeslets and eddies in creeping flow. *Ann. Rev. Fluid Mech.* **12**, 335–363.

Hirschfeld, B. R., Brenner, H. & Falade, A. 1984 First- and second-order wall effects upon the slow viscous asymmetric motion of an arbitrarily-shaped, -positioned and -oriented particle within a circular cylinder. *PhysicoChem. Hydrodyn.* **5**, 99–133.

Jeffery, G. B. 1915 On the steady rotation of a solid of revolution in a viscous fluid. *Proc. Lond. Math. Soc.* **14**, 327–338.

Ladenburg, R. von 1907 Über den Einfluss von Wänden auf die Bewegung einer Kugel in einer reibenden Flüssigkeit. (On the influence of walls on the motion of a sphere in a viscous fluid.) *Ann. der Physik* **23**. 447–458.

Lamb, H. 1932 *Hydrodynamics* (6th edn), pp. 595–596. Cambridge University Press.

Leal, L. G. 1980 Particle motion in a viscous liquid. *Ann. Rev. Fluid Mech.* **12**, 435–476.

Lee, S. H. & Leal, L. G. 1980 Motion of a sphere in the presence of a plane interface. II. An exact solution in bipolar coordinates. *J. Fluid Mech.* **98**, 193–224.

Lee, S. H. & Leal, L. G. 1982 The motion of a sphere in the presence of a deformable interface. 2. Large deformations for motion normal to the interface. *J. Colloid Interface Sci.* **87**, 81–106.

Leichtberg, S., Pfeffer, R. & Weinbaum, S. 1976 Stokes flow past finite coaxial clusters of spheres in a circular cylinder. *Intl J. Multiphase Flow* **3**, 147–169.

Lorentz, H. A. 1896 A general theorem concerning the motion of a viscous fluid with some applications. *Zittingsverlag Akad. Wet. Amsterdam* **5**, 168–175; see also *Abhandlungen über theoretische Physik* Bd. **1**, S. 23–42, Leipzig 1907.

Majumdar, S. R. 1965 Ph.D. dissertation. Department of Mathematics, University of London.

Majumdar, S. R. 1967 Slow motion of an incompressible viscous liquid generated by the rotation of two spheres in contact. *Mathematika* **14**, 43–46.

Misner, C. W., Thorne, K. S. & Wheeler, J. A. 1973 *Gravitation*, pp. 509–516. Freeman.

O'Neill, M. E. 1964 A slow motion of a viscous liquid caused by a slowly moving solid sphere. *Mathematika* **11**, 67–74.

O'Neill, M. E. 1969 On asymmetrical slow viscous flows caused by the motion of two equal spheres almost in contact. *Proc. Camb. Phil. Soc.* **65**, 543–556.

O'NEILL, M. E. & MAJUMDAR, S. R. 1970*a* Asymmetrical slow viscous fluid motions caused by the translation or rotation of two spheres. I. The determination of exact solutions for any values of the ratio of radii and separation parameters. *Z. Angew. Math. Phys.* **21**, 164–179.

O'NEILL, M. E. & MAJUMDAR, S. R. 1970*b* Asymmetrical slow viscous fluid motions caused by the translation or rotation of two spheres. II. Asymptotic forms of the solution as the minimum clearance between the spheres approaches zero. *Z. Angew. Math. Phys.* **21**, 180–187.

O'NEILL, M. E. & RANGER, K. B. 1982 Particle fluid interaction. In *Handbook of Multiphase Systems* (ed. G. Hetsroni), pp. 1–96 to 1–183. Hemisphere/McGraw-Hill.

O'NEILL, M. E. & STEWARTSON, K. 1967 On the slow motion of a sphere parallel to a nearby plane wall. *J. Fluid Mech.* **27**, 705–724.

ROSENSWEIG, R. E. 1982 Magnetic fluids. *Scientific American* **247**, 136–145.

STIMSON, M. & JEFFERY, G. B. 1926 The motion of two spheres in a viscous fluid. *Proc. R. Soc. Lond.* A **111**, 110–116.

WEATHERBURN, C. E. 1927 *Differential Geometry of Three Dimensions*, pp. 61, 67. Cambridge University Press.